JPRS-CST-86-043

14 OCTOBER 1986

China Report

SCIENCE AND TECHNOLOGY

FBIS FOREIGN BROADCAST INFORMATION SERVICE

NOTE

JPRS publications contain information primarily from foreign newspapers, periodicals and books, but also from news agency transmissions and broadcasts. Materials from foreign-language sources are translated; those from English-language sources are transcribed or reprinted, with the original phrasing and other characteristics retained.

Headlines, editorial reports, and material enclosed in brackets [] are supplied by JPRS. Processing indicators such as [Text] or [Excerpt] in the first line of each item, or following the last line of a brief, indicate how the original information was processed. Where no processing indicator is given, the information was summarized or extracted.

Unfamiliar names rendered phonetically or transliterated are enclosed in parentheses. Words or names preceded by a question mark and enclosed in parentheses were not clear in the original but have been supplied as appropriate in context. Other unattributed parenthetical notes within the body of an item originate with the source. Times within items are as given by source.

The contents of this publication in no way represent the policies, views or attitudes of the U.S. Government.

PROCUREMENT OF PUBLICATIONS

JPRS publications may be ordered from the National Technical Information Service, Springfield, Virginia 22161. In ordering, it is recommended that the JPRS number, title, date and author, if applicable, of publication be cited.

Current JPRS publications are announced in Government Reports Announcements issued semi-monthly by the National Technical Information Service, and are listed in the Monthly Catalog of U.S. Government Publications issued by the Superintendent of Documents, U.S. Government Printing Office, Washington, D.C. 20402.

Correspondence pertaining to matters other than procurement may be addressed to Joint Publications Research Service, 1000 North Glebe Road, Arlington, Virginia 22201.

JPRS-CST-86-043

14 OCTOBER 1986

CHINA REPORT

SCIENCE AND TECHNOLOGY

CONTENTS

ABSTRACTS

SCIENTIFIC RESEARCH FUND REFORMS 'GOING SLOWLY'

HK150252 Beijing CHINA DAILY in English 15 Aug 86 p 1

[Report by staff reporter Xu Yuanchao]

[Text] China is to speed up nationwide reforms in the way funds are given to scientific research institutes as the key to restructuring the scientific and technical research system.

The reform is expected to be completed by the end of the year. Starting next year, the growth rate of funds allocated to research institutes throughout the country would exceed the growth of the national income, a conference held this week by the State Science and Technology Commission heard.

A commission official said the Ministry of Finance would allocate 1.4 billion yuan (excluding military appropriations) to research institutes (not including those in social sciences) in this fiscal year. Already, in the first half, about 800 million yuan had been granted.

The budget for research institutes this year had increased 6 percent over last year, compared with a 7.8 percent growth in the nation's revenue, he said.

Following a State Council decree early this year, the Ministry of Finance is to shift its power of fund allocation to the commission so as to make effective use of the limited funds.

But the official said the funds were enough only for small-scale researches. Large research projects would be "contracted by the state to research institutes through competitive bidding."

The research institutes will be divided into three categories.

--Technology development, pure research [word indistinct] welfare, which includes public health, labour protection, family planning, environment protection and disaster control.

Operating expenses for research institutes in technology development will be cut down during the current five-year plan (1986-90) to encourage them to bid for larger projects, the official said.

The projects are designated by the State to meet the current needs of the national economy. The funds saved from operating expenses will be used to make up investment in the country's priority projects, the official said.

The official said the reform was going slowly. About 50 percent of research institutes in local areas had not started the work and some were even taking a wait-and-see attitude.

But in the first half of this year, the reform had been basically accomplished among research institutes subordinate to central ministries and commissions.

/9604
CSO: 4010/2020

REFORM OF RESEARCH FUND APPROPRIATION URGED

OW251112 Beijing XINHUA Domestic Service in Chinese 0704 GMT 24 Aug 86

[Excerpt] Beijing, 24 Aug (XINHUA)--To speed up reforming the system of appropriating funds for scientific operations, the State Scientific and Technological Commission [SSTC] and the Ministry of Finance [MOF] have urged all provinces, regions, municipalities and counties that the transfer of such funds should be carried out simultaneously and completed by the end of this year. They say that beginning 1 January next year, funds for scientific operations should be placed under the management of various scientific and technological commissions, and in accordance with the new format of the MOF's new budgetary plan.

Reforming the system of appropriating funds for scientific operations is an important part of reforming the management of science and technology. So far, this reform has already been carried out in departments under the State Council. The funds for scientific operations of 53 departments have been transferred to the SSTC management, and the categorization of research projects of these departments' research organs has also been basically completed. However, the progress of reform is uneven in various localities. While some have started or are about to start, some others are still waiting. The SSTC and the MOF maintain that the time is ripe for reforming the appropriation system, and that tardiness will affect reforming the management of science and technology as a whole.

In a circular, the SSTC and the MOF have defined the scope of transferring local research funds to the management of local scientific and technological commissions, stating that research and operation funds (including operation funds for various scientific and technological associations) should be defrayed by the operation funds of various departments.

The SSTC and MOF circular points out that reforming the system of appropriating funds for scientific operations is key to reforming scientific and technological management and that all localities must intensify their leadership over the project. They say that scientific and technological commissions and financial departments at all levels should provide meticulous guidance on the basis of conducting investigation and study.

/9604
CSO: 4008/2131

NATIONAL DEVELOPMENTS

FIRST SCIENCE-TECHNOLOGY WHITE PAPER PUBLISHED

HK111551 Beijing RENMIN RIBAO in Chinese 10 Sep 86 p 1

[Report by Chen Zujia [7115 4371 3946]: "China Publishes First White Paper on Policies Concerning Science and Technology"]

[Text] "A Guide to China's Policies on Science and Technology--The First White Paper on Science and Technology," the first publication on China's principles and policies concerning science and technology and the implementation of these principles and policies, has come off the press and will go on sale across the country.

On 9 September, Wu Mingyu, vice minister of the State Science and Technology Commission, introduced the white paper to foreign scientific and technological officials, representatives of the United Nations offices in Beijing, representatives of foreign companies set up in China, and foreign and Chinese reporters and answered their questions.

A white paper is a government publication used by many countries to make public their major principles and policies of a certain period. With the approval of the State Council, China's white paper on science and technology gives an elaborate account of the main points, basis, and implementation of the principles and policies on science and technology formulated since the Third Plenum of the 11th CPC Central Committee. It carries important speeches made by party and state leaders during this period and the important documents and regulations promulgated by the CPC Central Committee and State Council.

The white paper consists of 6 sections and 26 chapters. Of this, the results of the 1985 national survey of science and technology, including the figures of the scientific and technological activities and personnel of the country's research and exploitation institutes, the preliminary plan for the statistical system of China's science and technology, and the technological policies for 12 fields including energy, communications, and transportation have been made public for the first time.

Wu Mingyu said that the publication of the first white paper by the State Science and Technology Commission with the approval of the State Council is the outcome of the policies of reform and opening up to the outside world.

China attaches great importance to policies, Wu continued, but we have seldom compiled the state policies of a period and made them public. By publishing the white paper, the masses can understand the policies and turn them into action. Moreover, the masses can take part in supervision and the state can obtain feedback. Furthermore, we can help friends of all countries understand China's policies and develop mutual cooperation.

It has been reported that the State Science and Technology Commission will regularly publish white papers in the days to come. The English-language version of the first white paper is expected to be available in the spring of 1987.

/9604
CSO: 4008/2131

PROBLEMS WITH MIDDLE-AGED SCIENTISTS REVEALED

OW130917 Beijing XINHUA in English 0631 GMT 13 Sep 86

[Text] Beijing, 13 Sep (XINHUA)--China has failed to take full advantage of the skills of one-ninth of its four million middle-aged scientists, according to a report in today's overseas edition of the PEOPLE'S DAILY.

The Communist Party paper urged that "effective measures" be taken to better use the scientists' abilities.

It quoted the results of a recent survey by an unnamed source of 30,000 scientists between 36 and 55 years old in 500 work units. China has more than four million scientists of this age group.

The paper blamed the problem on "poor working conditions," such as inadequate books and reference materials, out-of-date instruments and equipment and inadequate support staff.

Lacking assistants, the paper said, more than 12 percent of the senior scientists surveyed said they do work that could be done by less qualified technicians.

Unequal distribution of household responsibilities also impairs the work of some scientists, it said.

"Those who are women routinely have to spend atleast 3 hours a day on household chores--in addition to helping their children with their homework," according to the report. "Combined with the long commuting time many people have, the household situation has prevented many women scientists from having time to study on their own."

The paper called for more in-service training. More than two-thirds of the scientists surveyed said they had had no refresher courses for at least 2 years.

/9604
CSO: 4010/2020

S&T INFORMATION INSTITUTIONS, SERVICES EXPAND

OW131425 Beijing XINHUA in English 1409 GMT 13 Sep 86

[Text] Beijing, 13 Sep (XINHUA)--China now has 3,883 scientific and technical information institutions of various sizes, employing 68,000 people, a senior Chinese official disclosed here today.

Wang Tingjun, director of the Scientific and Technical Information Department of the State Science and Technology Commission, said, as affiliates of government departments, colleges, factories, enterprises and various localities, these information institutions have in the past 3 decades provided valuable services for the country's science and economy.

Information scientists and technicians of the Chang Jiang Transport Department provided 102 research findings in a 10-year period for China's largest water-conservancy project on the Chang Jiang--Gezhouba.

Their service helped save some 100 million yuan of investment and 900 tons of rolled steel, and was very valuable for selecting a correct plan for damming the river and protecting the sturgeon, a freshwater fish.

Scientific and technical information projects, institutions and individuals who have distinguished themselves in this regard will be commended at a national conference on information work slated to be held in mid-October, Wang Tingjun announced.

Beginning in 1956, Wang recalled, the Chinese Government formulated as a national policy the development of scientific and technical information indispensable to the social, economic, scientific and technical development of the nation.

With the implementation of the policy of economic restructuring and opening to the outside world, scientific and technical information institutions extended their services to fields other than science and technology.

More flexible forms and means of service have been introduced, and computerization has been much improved. Moreover, there has been an unprecedented growth of Sino-foreign exchanges in this regard.

Wang Tingjun expressed the hope that scientific and technical information institutions and libraries would coordinate their efforts and make the best use of the country's limited information personnel, financial resources and materials.

/9604
CSO: 4010/2020

YAN DONGSHAN ON POLICYMAKING ROLE OF CAS

HK150242 Beijing CHINA DAILY in English 15 Sep 86 p 3

[Text] The Chinese Academy of Sciences will be more active in organizing China's top scientists to contribute to the democratic and scientific policy-making sought by the Chinese leadership, said Yan Dongsheng, vice-president of the academy, at a meeting of the Technical Science Academic Division that opened yesterday.

He said that as the members of the academy are the most outstanding specialists and experts in China, they should participate in State policy-making as special counsellors.

So, for the first time, over 90 well-known academics from different fields, 40 government officials and 20 technical experts from local enterprises gathered together to compare notes on the current social, economic and scientific developments.

"We've invited officials from major government departments to report and join discussions at the meeting. We believe this will help our scientists know more about the level and needs of national development," Yan said.

According to Shi Changxu, director of the Technical Science Division, the academy will propose four main subjects for its members to deliberate on and provide advice for the government.

The subjects include the allocation and utilization of resources; development of infrastructure; high-tech research, urban and rural construction and environmental protection.

The academy expects the scientists will form special subject groups and raise their research projects during the 4 days of reports and discussions. After the meeting, the groups will set out on study and field inspections.

"We hope the scientists will bring out some valuable reports in a couple of years. Because we are at an experimental stage so far, we'll focus on a few subjects at present. In future, we'll expand the counselling into more fields," Yan said.

/9604
CSO: 4010/2020

REFORM OF GUANGXI RESEARCH ORGANIZATIONS DISCUSSED

HK271359 Nanning Guangxi Regional Service in Mandarin 1000 GMT 26 Jun 86

[Text] The regional CPC Committee Standing Committee has recently made a decision on consolidating and readjusting scientific research institutes of all categories throughout the region with the aim of overcoming the malpractices of the old scientific and technological systems. The goal is for scientific research to be closely linked with production and better serve economic construction.

In the consolidation and readjustment work, we must begin by reforming the system of appropriation of funds and thoroughly change the stage of eating out of the same big pot. In accordance with the orientation of their own work and with the characteristics of their own activities, the existing scientific research organizations will be divided into four categories:

The scientific research institutes of the technological development type must organize their income through the transfer of technology. During the Seventh Five-Year Plan period, each year they must gradually reduce their operating expenses appropriated by the state until they can completely stand on their own feet.

The scientific research institutes of the technology foundation type can mainly solve the problem of their funds by applying for funds for science.

Regarding the operating expenses of the scientific research organizations which belong to the type of technology foundations in the public interests and the type of scientific research in agriculture, the contract system will be implemented and the state will encourage them to vigorously organize income from other enterprises and regions.

Scientific research institutes in many categories can solve the problem of funds through different channels.

In the course of consolidating and readjusting scientific research organizations, regarding those scientific research units whose conditions are very poor and technological ability weak and which do not meet the requirements for a research institute, we must take resolute measures to abolish

those that should be abolished and to amalgamate those which should be amalgamated. At the same time, in the light of the needs of the development of the national economy of our region, we must suitably set up some scientific research organizations. All newly established scientific research organizations of the technological development type must, in the future, take the road of standing on their own feet in regard to funds.

/9604
CSO: 4008/2131

BRIEFS

GAINS IN JIANGSU S&T REFORM--From January to July this year, Jiangsu conducted a large-scale, general scientific and technological survey, the first ever since the founding of the PRC. At a provincial briefing on the survey on 18 August, Wu Xijun, member of the provincial party committee standing committee and chairman of the Provincial Scientific and Technological Committee, announced: Since the central authorities' decision on scientific and technological structural reform, Jiangsu's scientific and technological structural reform has healthily developed. Reform has enabled research and development organizations to promote increasingly closer lateral ties with enterprises. Various scientific research and production associations have sprung up like mushrooms. Reform has steadily invigorated research and development organizations. As a result, their incomes have greatly increased. Incomes in 1985 increased by 300 percent over 1983, amounting to 2.9 times the operating expenses allocated by the state in 1985. Reform has also promoted the rational circulation of scientific and technical personnel and readjusted and improved the structure of scientific and technical ranks. [Excerpt] [Nanjing Jiangsu Provincial Service in Mandarin 2200 GMT 18 Aug 86] /9604

CSO: 4008/2131

APPLIED SCIENCES

DESIGN OF NEW WIDEBAND MICROSTRIP 3 dB HYBRID RING

Beijing DIANZI XUEBAO [ACTA ELECTRONICA SINICA] in Chinese Vol 14, No 1, Jan 86 pp 120-122

[Article by Wang Shulian [3769 2885 6647], National Fu Jiang Machinery Plant;
Paper received April 1984, revised June 1985]

[Text] Abstract: A new structure of the phase-moved network and a simple method for designing a wideband 3dB hybrid ring circuit are presented. The circuit has better electrical performance over 40 percent frequency band and can withstand higher power. It is easier to fabricate and has a wider field of applications.

1. Introduction

The wideband hybrid ring shown in Figure 1 has its prominant strength.[1, 2] However, the reversed-terminal short-circuit coupling-line width designed from the existing design scheme is quite narrow, having a small slot and low tolerance for power. Thus it is fairly difficult to realize in terms of architecture. Therefore, a new circuit design approach has to be explored.

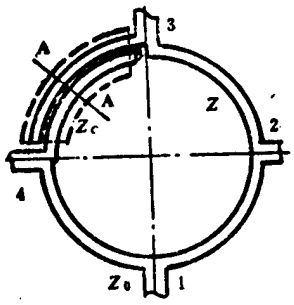

Figure 1. Circuit Diagram of a Wideband Hybrid Ring

At the present time, the reentry coupling theory has enjoyed extensive applications.[3, 4] Strong coupling 3dB wideband hybrid rings can be readily designed using this theory. The design presented in this article is a new design method combining the original hybrid ring design equations and the reentry coupling-line design theory.

2. Design Theory

The characteristic impedance of a $\lambda/4$ reversed-terminal short-circuit coupling line in the circuit shown in Figure 1 is:

$$Z_c = \frac{2Z_{oe}Z_{eo}\sin\theta}{[(Z_{ee}-Z_{eo})^2-(Z_{ee}-Z_{eo})^2\cos^2\theta]^{1/2}} \tag{1}$$

In order to maintain the overall phase move in the circuit at $180°+\theta = 270°$, let $\theta = 90°$. Then equation (1) is simplified as:

$$Z_c = 2Z_{oe}Z_{eo}/(Z_{ee}-Z_{eo}) \tag{2}$$

To have a matching transmission line between the coupling line and the other portions of the ring whose characteristic impedances are Zr, we must make:

$$Z_c = Z_r = \sqrt{Z_{ee}Z_{eo}} \tag{3}$$

The following is obtained when equations (2) and (3) are solved:

$$Z_{ee} = (\sqrt{2}+1)Z_r \tag{4}$$
$$Z_{eo} = (\sqrt{2}-1)Z_r \tag{5}$$

where $Zr = 1.46Z_O$, and Z_O is the input-output characteristic impedance.

For the 180° phase-moved network in Figure 1, the circuit width W and coupling slot S designed using equations (4) and (5) are particularly small. For instance, when the medium material $\varepsilon_r = 9$ and the board height H = 1mm, a ring width W = 0.12 mm and slot S = 0.04 mm are derived. This kind of hybrid ring can only be obtained using relatively advanced technology.

It is well known that the odd- and even-mode phase velocities for a microstrip coupling line are different, especially in the case of tight coupling where there is a drastic difference between the odd-mode impedance and the even-mode impedance. This is the primary reason why the aforementioned circuit architecture is difficult to realize. In order to solve the conflict whereby the odd-mode phase velocity is different than even-mode, phase velocity[5], a non-ground contact conductor (called suspension conductor for short) is introduced between the two coupling lines and the ground. The construction is as shown in Figure 2. The equivalent circuit odd and even mode impedance relationship of such coupling line is:

$$Z_{oo} = Z'_{oo} \tag{6}$$
$$Z_{oe} = Z_{01} + 2Z_{02} \tag{7}$$

where Z_{01} is the even-mode impedance corresponding to the odd-mode impedance Z_{00} at selected coupling slot S/H value; Z_{02} is the even-mode impedance formed between the suspension conductor and the ground. The familiar coupling-line impedance approximation equation can be of assistance in the solving for Z_{01}. The computation equation[6] is:

For odd-mode impedance $$Z_{oo} = \frac{\eta}{\sqrt{\varepsilon_r}} \cdot \left(C'_{oo} / \frac{\varepsilon_r}{c\eta} \right)^{-1} \tag{8}$$

For even-mode impedance $$Z_{oe} = \frac{\eta}{\sqrt{\varepsilon_r}} \cdot \left(C'_{oe} / \frac{\varepsilon_r}{c\eta} \right)^{-1} \tag{9}$$

where

$$C'_{oo} = C_{pp} + \frac{1}{2}(C_{ppv} + C_F + C'_F + C'_{ppv}), \quad C_F = \frac{\varepsilon_r}{c\eta} \cdot 2.7/\lg\frac{4H}{t}$$

$$C'_{oe} = C_{pp} + \frac{1}{2}(C_{ppv} + C_F + C''_F + C''_{ppv}), \quad C'_F = \frac{\varepsilon_r}{c\eta} \cdot 2.7/\lg\frac{4S}{\pi t}$$

$$C''_F = \frac{\varepsilon_r}{c\eta} \cdot 2.7/\lg\frac{4H}{t}\left(\frac{W}{S} + 1\right)^{-1}, \quad C_{pp} = \frac{\varepsilon_r}{c\eta} \cdot \frac{W}{H}$$

$$C_{ppv} = \frac{\varepsilon_r}{c\eta} \cdot \frac{2}{3\sqrt{\varepsilon_r}}\left[\frac{W}{H} - \left(\frac{W}{H} + 1\right)^{-2}\right]$$

$$C'_{ppv} = \frac{\varepsilon_r}{c\eta} \cdot \frac{8}{3\sqrt{\varepsilon_r}} \cdot \left(\frac{S}{W} + 1\right)^{-1}, \quad C''_{ppv} = \frac{\varepsilon_r}{c\eta} \cdot \frac{2}{3\sqrt{\varepsilon_r}} \cdot \frac{W}{H} \cdot \left(\frac{W}{S} + 1\right)^{-1}$$

When the S/H value has been selected, Z_{01} can be obtained using equations (8) and (9). However, it is fairly cumbersome to arrive at the result. To deal with the calculation, a computer-aided design is used. Programs (omitted here) are written for expressions (8) and (9) which represent the microstrip odd- and even-mode impedances for various media and various coupling slots S. The results are printed on a table (only the sample design Table 1 is given in this article). In doing so, the geometric size of the coupling line can be obtained very conveniently. The value for the impedance Z_{02} between the suspension conductor and the ground can be obtained from equation (7), and the geometric size of the suspension conductor can be further looked up using the table for single microstrip.

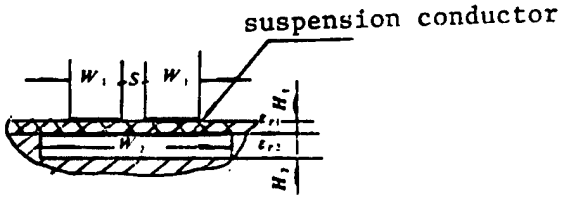

Figure 2. A-A Cross-sectional View from Figure 1

3. Design Computation and Experimental Results

A wideband microstrip 3dB hybrid ring is to be signed. The substrate material used is polytetrafluorethylene whose εr = 2.55, H = 1.5 mm, t = 0.05 mm, and Z_0 = 50 Ω. The design steps are as follows:

(1) Compute the odd- and even-mode impedances according to equations (4) and (5)

$$Z_{oo} = (\sqrt{2} - 1)Z_r = 30.24\Omega$$

$$Z_{oe} = (\sqrt{2} + 1)Z_r = 176.24\Omega, \quad Z_r = 1.46Z_0$$

(2) Calculate the coupling line size.

Select S/H = 0.5. Let H_1 = 1.5 mm, then S = 0.75 mm. When Table 1 is looked up, as W_1/H_1 = 4.25 corresponding to Z_{00} = 30.24 Ω, and as H_1 = 1.5 mm, then W_1 = 6.38 mm. In addition, the even-mode impedance Z_{01} corresponding to Z_{00} is looked up as 39.3 Ω.

(3) Compute the suspension conductor to ground impedance Z_{02} from equation (7).

$Z_{02} = (Z_{00} - Z_{01})/2 = 68.46\Omega$, from Table 1, suspension conductor width W_2/H_2 = 3.13. Pick H = 6 mm, then W_2 = 18.78 mm.

(4) Compute λs/4 and the diameter of the ring

$\lambda_g/4 = \lambda_0/4\sqrt{\varepsilon_e}$, λ_0 is the space wave length, λg is the medium wave length, and ε_e is the equivalent dielectric constant.

Table 1. Coupling-line Characteristic Impedance (ε_r = 2.55)

S/H	W_1/H_1	Z_{00}	Z_{01}	Z_{02}	W_2/H_2
0.4	4.14	30.24	40.32	67.96	3.17
0.5	4.25	30.24	39.3	68.46	3.13
0.6	4.32	30.24	38.54	68.84	3.10

Figure 3 shows the following: signals fed into opening no. 1, output amplitude A from opening nos. 2 and 4, interval I at opening no. 3, the voltage standing wave ratio (VSWR) for the four openings, and equiphase input and reversed phase input into opening nos. 2 and 4 as well as the output phase ϕ.

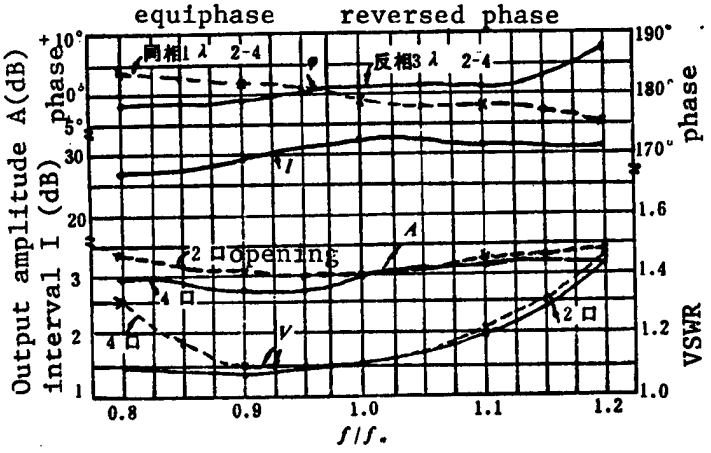

Figure 3. Curve of Output Amplitude A, Interval I, VSWR V and Phase φ Against Changing Frequency

4. Conclusion

The circuit described in this article has a better electrical performance compared with the hybrid ring whose circumferential length is 1.5 wavelength. Approximately over 40 percent of the frequency band, the voltage standing-wave ratio at each opening is less than 1.5, output amplitude A = -3 ± 0.5 dB, interval I > 27 dB, the output phase in equiphase case is less than ± 5°, and the output phase in reversed phase case is less than ± 10°.

As a result of the innovation in architecture and circuit design approach which overcomes the fatal weakness in the original circuit having a small line width, narrow slot, and low tolerance for power, the new microstrip hybrid ring enables a wider application for the original hybrid ring.

Appreciation is extended to two very helpful comrades, Luo Yuping [5012 3768 1627] and Lai Xiaoya [6351 1420 7161].

REFERENCES

1. Harlan Howe, Jr., "Stripline Circuit Design," Artech House, Inc., 1974, pp 85-94;

2. S. March: IEEE TRANS, Vol MTT-16, 1968, p 361.

3. Lin Weigan [2651 3634 1631], "Microwave Network," National Defense Industry Publishing House, 1978, pp 211-219, 271-276;

4. Yin Liansheng [3009 6647 3932], "Analysis and Design of a Reciprocal Recoupling Microstrip 3dB Electric Bridge," Transmission Line Edition, by the Radar Information Editing and Translation Group of the Nanjing Electronic Technology Institute, 1978, pp 34-40;

5. Chen Zhencheng [7115 2182 2052], "Microstrip Serial Fed Power Distributors/-Synthesizers," ACTA ELECTRONIC SINICA, 1984, No 3;

6. Gu Qizheng [7357 0366 6154] et al., "Microwave Integrated Circuit Design," People's Posts and Telecommunications Publishing House, 1978, pp 45-64.

13042/7358
CSO: 4008/1088

ENVIRONMENTAL EFFECTS ON COMPUTER-CONTROLLED FEEDING SYSTEM

Shanghai ZIDONGHUA YIBIAO [PROCESS AUTOMATION INSTRUMENTATION] in Chinese
Vol 7, No 5, 20 May 86 pp 30, 38

[Article by Tong Suqin [0157 4790 5367], He Suzhi [0149 4790 5347], and Lin Lu [2651 0712], Anshan Ion Smelting Plant]

[Text] In October 1983, the Shanghai Process Automation Instrumentation Institute successfully developed a computer-controlled feeding system for the No 10 blast furnace in our plant. Ever since it has been in operation, this system has demonstrated steady performance, realizing precision coke/ore measurement with prominent economic benefits and contributing to a reduction in the rate of coke consumption as well as energy conservation.

1. Basic Function of the System

The industrial computer used in the No 10 blast furnace is used to control the ore in the blast furnace such as the loading amount and pre-load amount and to compute the ore and coke weight compensation and coke moisture compensation. The computed results are passed to the sequence controller by the computer, loading the coke and ore into the blast furnace using loading carts.

If there were fluctuations in the blast furnace, the blast furnace foreman would modify the predetermined value, the compensation value, and the pre-load amount relating to loading on the computer's keyboard, bringing the blast furnace to a stable state. (Generally, the loading of the furnace could be brought to a stable state primarily by adjusting the pre-load amount.) The printer provides data regarding shift and daily accumulations, coke moisture value, batch weight, and so on.

2. Environmental Effects on the System and the Solutions

The environment in which the blast furnace instruments are used is extremely unfavorable. The signal input to the computer is delivered from the transducer which is installed under the furnace ditch and is subject to high temperature, vibration, and electroconducting dust as well as the interference magnetic field influence that arises from the frequent turning on of large-scale electric machinery. In the case of a computer into which micro-signals are fed, a significant fluctuation can result from very small interference and will directly affect the operation of the computer.

(1) Influence from Environmental Temperature and the Solution

The device used in our plant is a LGA-high precision transducer manufactured by the Hangzhou Measuring Instrumentation Plant with the following specifications. The operating temperature is -10 ~ + 40°C, internal resistance is 350 Ω, the rated non-iterations for both the nonlinear and the lag are less than +0.03 percent, with an error of less than 0.05 percent for the three combined, and the responding plate is made of a cobalt-nickel alloy.

An illustration is presented as follows using the transducer in the ore scale as an example. In July 1984, the blast furnace foreman discovered that the ore-loading amount accumulated by the computer was much higher than the theoretical amount based on the furnace ion yield computation. The cost of pig ion would increase when this phenomenon occurred. Initially, we suspected damage in the transducer which turned out all right after the diagnosis. The working temperature of the transducer during that period was 65°C (due to the high temperature caused by thermal radiation from heating the ore). Because the temperature exceeded the specified temperature for the transducer, the transducer's temperature self-compensated resistance failed. The sensitivity coefficient of the responding plate changed with the fluctuation in temperature, resulting in an increase in the load for the transducer. The output signals from the transducer followed the increased load which was not a linear increase.

We covered the transducer with a square box we made from metal sheeting. Compressed air at a constant temperature was passed into the box. (In case conditions did not permit it, the transducer was relocated far from the middle bin where ore is loaded, as well as far from the conveyor on which the ore is transported, as a measure against thermal radiation.) In doing so, not only can it be assured that the transducer will be working under constant temperature, but the electro-conductive dust can also be avoided. Practical experience has proved that it is a better approach.

(2) Influence from Vibration and the Solution

The No 10 blast furnace is a relatively large blast furnace with a feed of 12-14 tons per load from the cart. Fierce vibrations would result when the scale was loading the feed. Because of the influence of vibration, the output signals from the transducer were unstable, the useful lifetime of the transducer could be shortened, and measurement errors could increase. Therefore, a certain amount of time has to be reserved in software programming regarding sample collection so that signals can only be read into the computer after the output signals from the transducer have been stabilized.

In order to assure accuracy in the measurements, the prolonged useful life of the transducer, and stable output signals from the transducer, as well as to minimize the computer's operating time, we employed the following measures:

a) The machine's zero weight must be accurate. Minimize when at all possible the pre-tension of the transducer at empty load;

b) Add a stage mechanical drive lever to achieve the buffering against the scale (as shown in Figure 1);

c) Output the data from the computer after the output signals from the transducer have been stabilized; and

d) Add anti-vibration padding to the transducer's steady voltage supply.

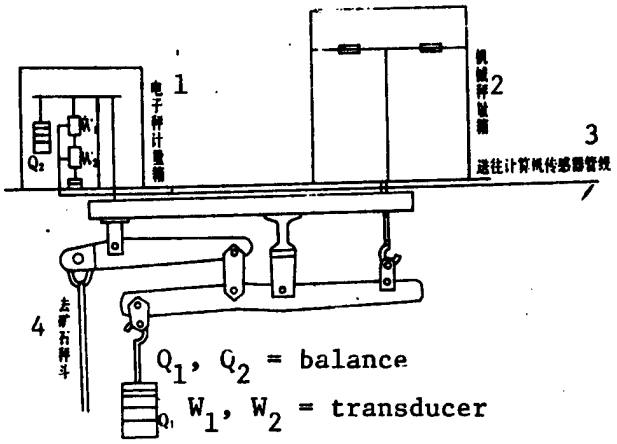

Figure 1

Key:
1. Electronic balance measurement box
2. Mechanical balance measurement box
3. Line feeding to the computer transducer
4. To the ore scale

(3) Electromagnetic Influence and the Solution

(a) Method to eliminate space induction interference

The frequent on and off of large-scale electric machinery is the primary factor producing space induction. To solve this problem, when the utility room for our plant was built, shielding screens were installed, and the ground contact points for such equipment as the transducer, steady voltage supply, and sequence controller were installed as far as possible from the ground contact point of the computer. Practical experience has proved that the result was very good.

(b) Method to eliminate interference from current supply system

A steady AC voltage supply source and an isolating transformer were employed to prevent the influence on the computer from electrified wire netting. The steady voltage current supply for the transducer was provided by the steady

AC voltage supply, as shown in Figure 2. In so doing, electrified wire netting was basically radicated.

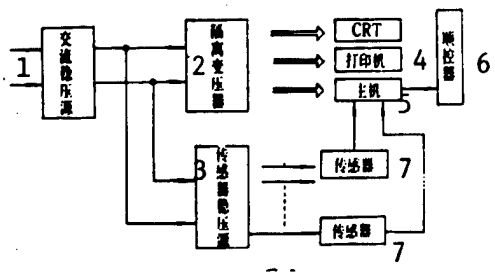

Figure 2

Key:

1. Steady AC voltage supply
2. Isolating transformer
3. Steady transducer voltage supply
4. Printer
5. Computer
6. Sequence controller
7. Transducer

13042/7358
CSO: 4008/1103

RESEARCH ON HIGH-GAIN BROADBAND BACKFIRE ANTENNA

Beijing DIANZI KEXUE XUEKAN [JOURNAL OF ELECTRONICS] in Chinese Vol 8, No 3, May 86 pp 223-227

[Article by Song Ximing [1345 6932 2494] of the Huanghe Machine Building Plant; received 18 September 1984, revised 6 September 1985]

[Text] I. Brief Review

Recently, there have been various theoretical analyses and physical explanations regarding the high-gain radiation characteristics possessed by a backfire antenna. However, the schools are different. This article is based on the basic theory given in Reference [1]: the backfire antenna is approximately equivalent to the antenna of a concaved reflector. In addition to the "equivalent focal point" and "equivalent focal distance," it also has the following relational equation:

$$\left.\begin{aligned} f &= n\lambda, \\ R &= \sqrt{n+\frac{1}{4}}\,\lambda, \end{aligned}\right\} \quad n = 1, 2, 3, \cdots\cdots, \qquad (1)$$

where f is focal distance and R is the radius of the surface wave reflector. Optimal gain is obtained when the phase center of the feeding source is at the equivalent focal point. The following corollaries can be obtained from Equation (1):

Corollary 1. For different values in n:

$$\begin{aligned} n &= 1, \quad f = \lambda, \quad R \approx 1.12\lambda; \\ n &= 2, \quad f = 2\lambda, \quad R \approx 1.50\lambda; \\ n &= 3, \quad f = 3\lambda, \quad R \approx 1.80\lambda; \\ n &= 4, \quad f = 4\lambda, \quad R \approx 2.10\lambda; \\ &\vdots \qquad\quad \vdots \qquad\quad \vdots \end{aligned}$$

then for a given n value, the optimal radiation characteristic can only be obtained under the corresponding f and R.

Corollary 2. There are n "equivalent focal points/distances" for the backfire antenna. However, corresponding to the surface wave reflector having the above given radius, the optimal radiation characteristics can only be obtained when the phase center of the feeding source is at the corresponding focal point.

Corollary 3. The "equivalent focal point/distance" of the backfire antenna is a function of frequency, changing with the frequency. Assume the presence of a feeding source whose phase center is also a function of frequency and whose functional format is the same as or similar to the functional format of the "equivalent focal point/distance," then a broadband backfire antenna can be obtained when such a feeding source is taken as the backfire antenna's feeding source.

Based on the above corollaries, we design several backfire antennas to perform experimental research.

II. Experimental Results

1. High-gain backfire antenna

For the backfire antenna experimental model (please refer to Figure 1 of Reference [1]), the radii of the surface wave reflectors are 1.12λ, 1.5λ, 1.8λ, and 2.1λ, respectively; the rim height can be adjusted continually from $0\text{-}2\lambda$; the radius of the small reflector is 0.5λ - 1.0λ; and the feeding source is a half wave oscillator. In addition, a transfer equipment of slot-eqioaxle balance-imbalance is employed. The experiment is conducted in an open outdoor field.

(1) Antenna performance at different values of n

An experiment is performed on antennas of different sizes. Their typical directional diagrams under the optimal radiation states are shown in Figures 1, 2, 3, and 4, respectively. At this point, their corresponding measured gains are 17.5 dB, 19.2 dB, 20.8 dB, and 23 dB, respectively.

It can be seen from the experimental results that the antenna's radiation characteristics is in closer agreement with Corollary 1. As the measured gains are reviewed, if one is to use $G = 4\pi S_A/\lambda^2$ to do the estimate, the effective aperture area S_A of the antenna exceeds the actual geometric area in some cases (such as n = 1 and 4). (Of course, the influence from the rim is not taken into consideration here. As for the function of the rim, i.e., the discussion on "effective aperture radius gain," please refer to Reference [1].) It is an indication that the efficiency of the antenna is pretty high.

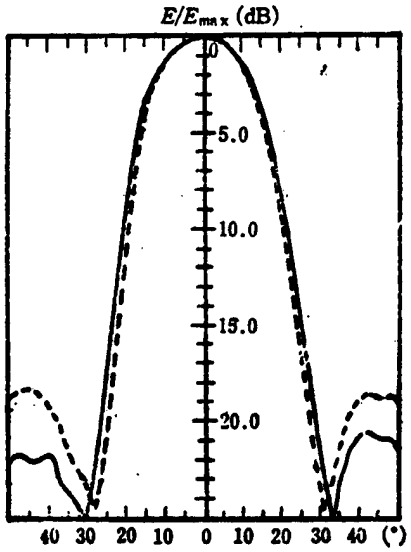

Figure 1. Experimental Direction Diagram at n = 1

----- Vertical polarization

..... Horizontal polarization

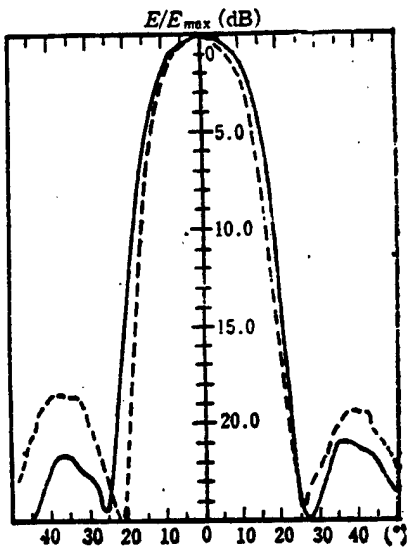

Figure 2. Experimental Direction Diagram at n = 2

----- Vertical polarization

..... Horizontal polarization

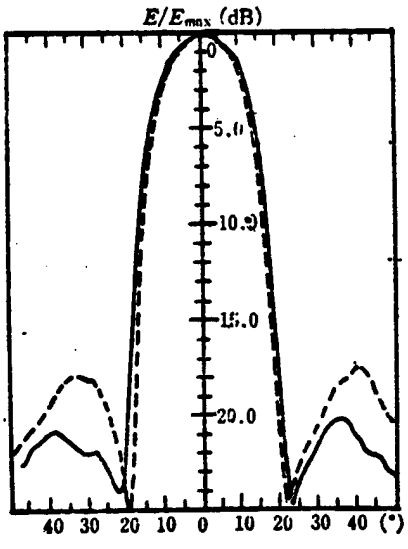

Figure 3. Experimental Direction Diagram at n = 3

----- Vertical polarization

..... Horizontal polarization

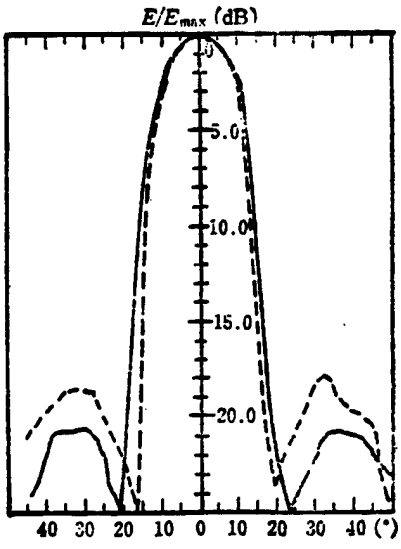

Figure 4. Experimental Direction Diagram at n = 4

----- Vertical polarization

..... Horizontal polarization

(2) Relationship between the feeding source and radiation characteristics

According to Corollary 2, if n = 1, 2, and 3 are taken respectively, the radii of the surface wave reflectors are 1.12λ, 1.5λ, and 1.8λ, respectively. The longitutional position of the feeding source can change continually within a certain range; then the relationship curve representing the received power of the designed antenna and the position of the feeding source can be seen as shown in Figure 5. It can be seen from the figure that the way the curve changes is in agreement with Corollary 2.

This type of antenna is insensitive to polarization and capable of resulting in linear polarization and oval polarization (circular polarization). If a cross-shaped oscillator is used as the feeding source and is placed at the optimal position, then at the direction on which the value of the wave beam is the greatest, the measured axle ratio when frequency is f_0 is less than 0.3 dB. However, a poorer axle ratio will result if a cylindrical spiral wire is used as the feeding source.

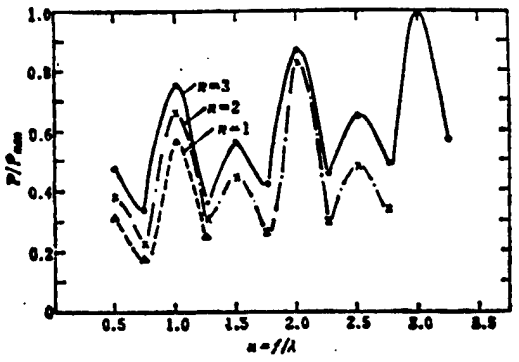

Figure 5. Effect of Position of Feeding Source on Gain

2. Broadband backfire antenna

It is well known that one of the major drawbacks of the backfire antenna is its relatively narrow working band, with a band width only reaching to 10 percent, approximately. Based on Corollary 3, and using a cone-shaped spiral antenna as the feeding source, we design a broadband backfire antenna which has better radiation characteristics with a 50 percent relative bandwidth.

We understand that the cone-shaped spiral wire is formed with a group of coils (about 3.5-4 wraps). The length of each round in the coil approximately equals the wave length at the center frequency (varying within the range of 0.8-1.3λ, where λ is the wave length in free space). These coils work under the state similar to the cylindrical spiral-axle radiation state. Inside this group of coils, the T_1 wave is the most significant. At the high-frequency end of the frequency band, those coils located at the smaller radius spiral wire are contributing, whereas at the low-frequency end of the frequency band, those coils located at the larger radius spiral wire are contributing. In the middle of

the frequency band, it is those coils located at the center of the spiral wire that contribute. Thus, the antenna is capable of working inside a fairly wide frequency band. Of course, although the rest of the coils do not contribute significantly, however, there is still some weak radiation which has some influence on the shape of the radiation direction diagram.

The frequency band we experiment with is 1,600-2,900 MHz, with a relative band width of 50 percent, approximately. The spiral antenna is constructed using red copper pipe whose diameter is 3 mm.

The experimental direction diagram inside the working frequency band is shown in Figure 6. It can be seen from the figure that the antenna has better radiation characteristics inside the frequency band; the width of the half-power point on the direction diagram shrinks with increasing frequency. In addition, the corresponding axle ratio is given in the figure. The input voltage standing-wave coefficient of the antenna inside the frequency band is less than 2.5, and is less than 1.50 in 25 percent of the band width.

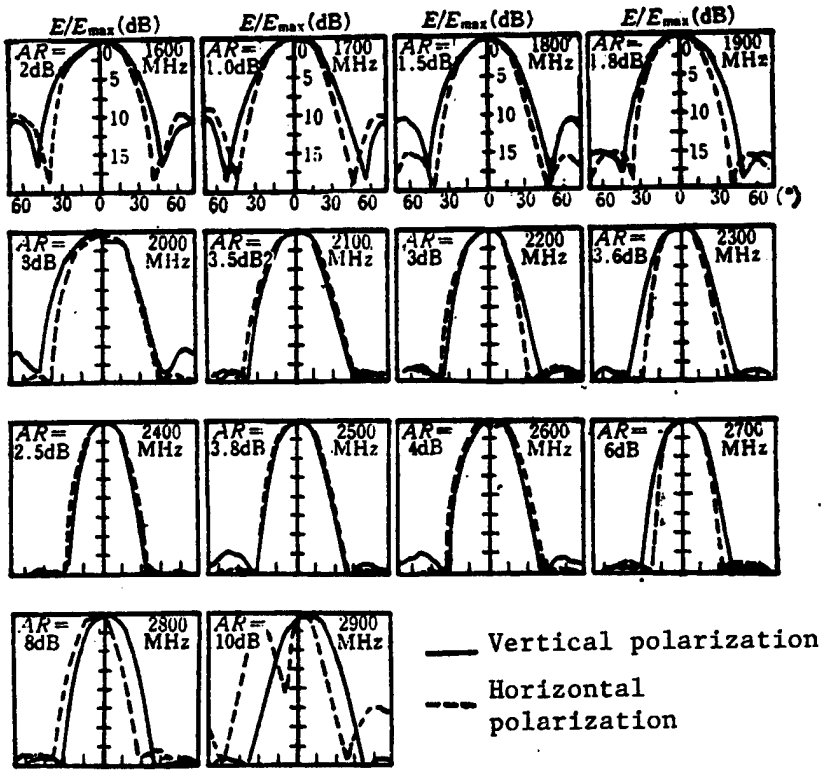

Figure 6. Experimental Direction Diagram

P_{max} is the maximum receiving power at n = 3.

It is noted in the experiment that the height of the rim has an effect on the antenna's radiation characteristics, and such an effect is more significant on the auxiliary amella electricity level. The size and the position of a smaller reflector have more significant influence on the performance of an antenna. In general, better radiation characteristics can be obtained when the diameter of a smaller reflector is set at 0.5λ.

If a disk of proper size is introduced between the surface wave reflector and the cone-shaped spiral wire, and after fine tuning, it can improve the antenna's performance significantly, especially in the enhancement in axle ratio. However, at the same time, the working frequency band would become much narrower.

III. Conclusion

(1) An "equivalent focal point/distance" indeed exists for the backfire antenna. The optimal radiation characteristics of the antenna can be obtained when the phase center of the feeding source is located at the equivalent focal point.

(2) The backfire antenna designed from the theory proposed in Reference [1] possesses the best radiation characteristics.

(3) A broadband backfire antenna can be designed based on the theory given in Reference [1].

(4) This article is an experimental support verifying the theory regarding the backfire antenna given in Reference [1].

This project received the dedicated guidance from Associate Professor Lin Changlu [2651 2490 4389] of the Chengdu Telecommunication Engineering College. In addition, a great portion of the experiment work was completed with the assistance from Comrades Rao Boliang [7437 0130 5328], Li Ruihua [2621 3843 5478], and Zhang Yufeng [1728 3768 1496]. Our appreciation is extended to all of them.

BIBLIOGRAPHY

1. Lin Changlu [2651 2490 4389] and Song Ximing [1345 6932 2494], DIANZIXUE TONGXIN [ELECTRONICS BULLETIN], No 4, 1982 p 331.

2. Lin Changlu [2651 2490 4389] and Song Ximing [1345 6932 2494], "1983 International IEEE/APS Symposium and National Ratio Science Meeting at the University of Houston," pp 138-141.

3. Lin Changlu [2651 2490 4389], CHENGDU DIANXIN GONGCHENG XUEYUAN XUEBAO, [CHENGDU TELECOMMUNICATION ENGINEERING COLLEGE JOURNAL] No 10, 1979 pp 97-102.

4. A.Z.Fradin, "Superhigh Frequency Antenna," translated by Chen Bingchun [7115 4426 6874] and Xiao Duchi [5135 4648 1062], International Industry Publishing House, 1962, Chapter 11.

13042/7358
CSO: 4008/1101

PMR TYPE AMIDE-IMIDE POLYMER, COMPOSITES

Beijing GAOFENZI TONGXUN [POLYMER COMMUNICATIONS] in Chinese No 3, Jun 86 pp 219-225

[Article by Zhu Wenjiang [2612 2429 3068], Zhang Chongli [1728 1504 4539], and Huang Zhitang [7806 1807 6974], Beijing Institute of Chemistry, Chinese Academy of Sciences; Paper received 27 May 1984; presented at the 1983 Hangzhou Polymer Symposium]

[Text] Abstract: The "PMR" (polymerization of monomer reactants) type polyamide-imide resins were prepared from bicyclo-[2.2.1]-hept-5-ene-2,3-dicarboxylic acid monoethyl ester, 1,2,4-trimellitic acid 2-(or 1-) ethyl ester, and 4,4'-diaminodiphenylmethane in ethanol. The composites fabricated from these resins can be used at 260°C over an extended period. The mechanism of formation of polyamide-imide was studied by using model compounds.

Aromatic polyamide-imides (PAI) are generally prepared by condensation polymerization of trimellitic anhydride 4-acyl chloride and aromatic diamines in highly polar, non-protic solvents (e.g., DMF).[1] Materials made from the polymer are viscosity- and heat-stable and are good insulators. But it is not suitable for composite application because of its high molecular weight. Although efforts have been made in improving molecular weight and in finding better starting materials, no significant results are accomplished.[2] It has recently been reported[3] that the amide-imide polymer prepared by using maleic anhydride as a capping reagent shows good flexural strength. However, the resin preparation process involves a high-boiling, toxic solvent and its high molding pressure limits to a certain extent, has wider applications. Based on our experience with the "PMR" type polyimide capped by bicyclo-[2.2.1]-hept-5-ene-2,3-dicarboxylic anhydride (NA), we studied the "PMR" type polyamide-imide resins. The preparation of the resin solution was carried out again in ethanol, using trimellitic anhydride (TMA) and 4,4'-diaminodiphenylmethane (M) as starting materials. Bicyclo-[2.2.1]-hept-5-ene-2,3-dicarboxylic ethyl ester (N) and 1,2,4-trimellitic acid 2- (or 1-) ethyl ester (T) were prepared in anhydrous ethanol. The "PMR" solutions of polyamide-imide of various "molecular weight" were then rpepared in ethanol. In this paper, we mainly studied the amidation reaction at the 4 position and the imidization and amidation reactions at 1 and 2 positions of 1,2,4-trimellitic acid 2-ethyl ester. The structures of low molecular weight polymer and the technology and properties of composite materials were investigated and discussed.

Results and Discussion

1. Amidation of 4-Carboxyl Group of Compound T

The NA-capped "PMR" type PAI resin solution exists as amine salt and can be written as follows:

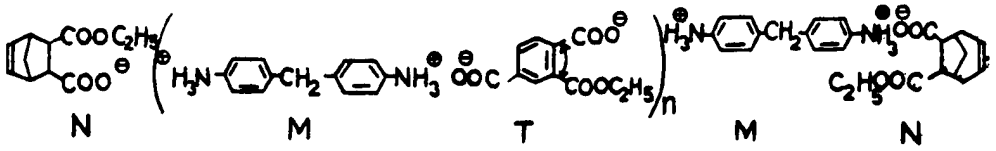

N M T M N

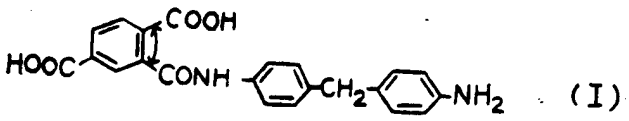

(I)

N-(-M—T-)$_n$M—N

In the previous paper,[4] it was pointed out that compound N reacts readily with M. Therefore, the key questions in PAI synthesis are under what condition and by what mechanism different carboxyl and ester groups on compound T react with M. Considering the electronic effect, 4-carboxyl group is much less acidic than 1- and 2-carboxyl groups (two orders of magnitude less). Obviously, 4-carboxyl group is less reactive and less likely to undergo amidation with an amino group. Our experimental results show that no 4-position reaction product formed when compound T, aniline, p-aminobipheny, and compound M were reacted at 150°C for 1-4 hours. All products are 1- or 2-position derivatives. It is also reported in the literature[3] that only 80 percent of 4-position carboxyl group undergo amidation after 28 hours at 200°C. In order to establish the effect of reaction temperature on the amidation of 4-position carboxyl group, we measured the DTA trace of model compound I (Figure 1). The results show that the amidation temperature of 4-carboxyl is around 230°C whereas those of 1- and 2-carboxyls are about 170°C.

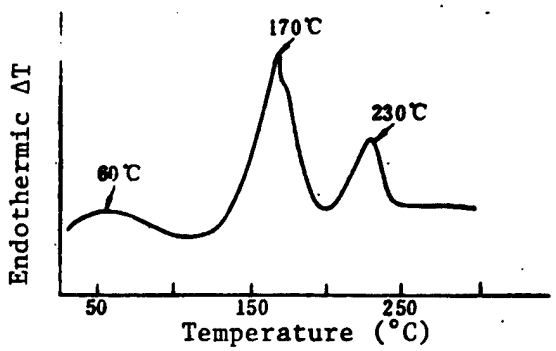

Figure 1. DTA Trace of Compound I

To confirm further the extent of amidation of the 4-carboxyl group, we again use compound I as a model to determine, as an indicator of the extent of amdiation, changes in these carboxyl groups after reacting at different temperatures over a certain period of time. It can be seen from Table 1 that the complete amidation of the 4-carboxyl group of compound I takes 3-4 hours at 250°C or 1 hour at 280°C.

	200℃/1h	230℃/1h	250℃/1h	250℃/2h	250℃/3h	250℃/4h	280℃/1h
Percentage of reacted 4-carboxyl group	24.1	68.9	77.0	95.0	97.9	99.3	99.3

Table 1. Extent of Amidation of Compound I

2. Amidation and Imidization of 1- and 2-position Carboxyl and Ester Groups of Compound T

As pointed out earlier, when compound T is treated with such aromatic amines as aniline at 150°C, 1- and 2-carboxyl groups react completely. How are amide and imide formed from this ester ammonium salt? On the one hand, the salt can be dehydrated at a high temperature to form amide ester, which then forms imide by ethanol elimination (Equation 1), namely by the nucleophilic addition of amino group through its line pair electrons to the carbonyl carbon of the carboxyl group. On the other, the carboxyl and ester groups at positions 1 and 2 can form anhydride upon heating by losing a molecule of ethanol through a cyclic intermediate, an endothermic process. It then forms amide acid and imide (Equation 2).

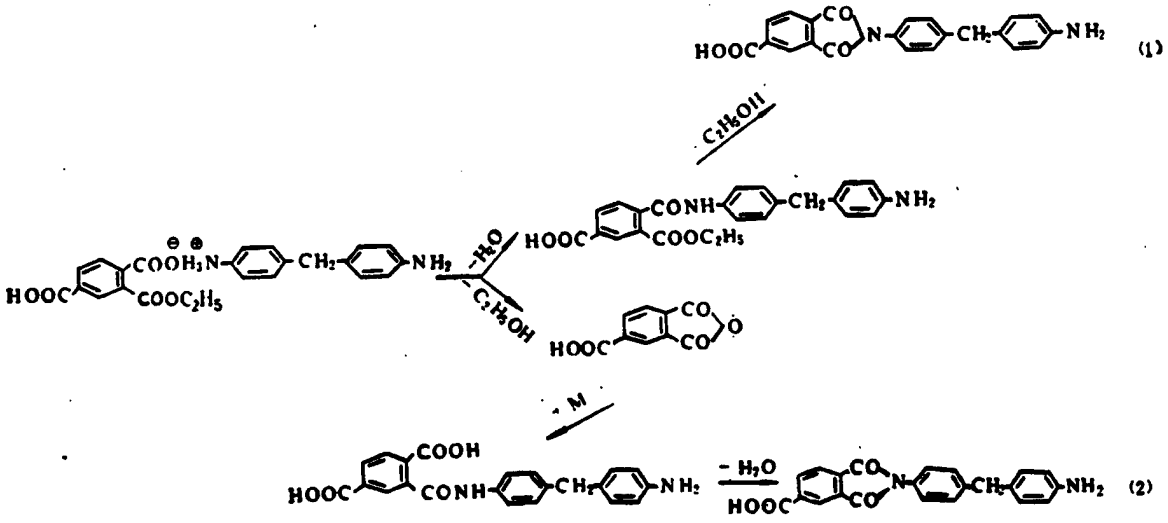

It is well known that the dehydration reaction in Equation 1 to form amide can only be accomplished at high temperature and the resulting amide ester requires an even higher temperature to form imide through the elimination of ethanol. This contradicts the experimental observation that imide can be formed at below 150°C. If the reaction follows Equation 2, we try to confirm it by the heating experiment on compound T. But the results show that after heating compound T at 150° and 200°C, the yields of anhydride are 2 and 18 percent, respectively. Obviously, this also does not agree with the above observation that imidization occurs readily. So both mechanisms (1) and (2) cannot account for the experimental results. For this reason, we prepared compound II, m.p. 113°C, and measured its TGA/DTA diagram (Figure 2) by thermal analysis. The results show that there appear three weight loss regions a, b, and c in the TGA diagram. The region b is located in the 140°-170°C range, not far from the m.p. A large endothermic peak and a higher weight loss rate (10.8 percent) occur within this region. The weight loss rate is very close to the theoretical value for the loss of one ethanol molecule (10.13 percent).

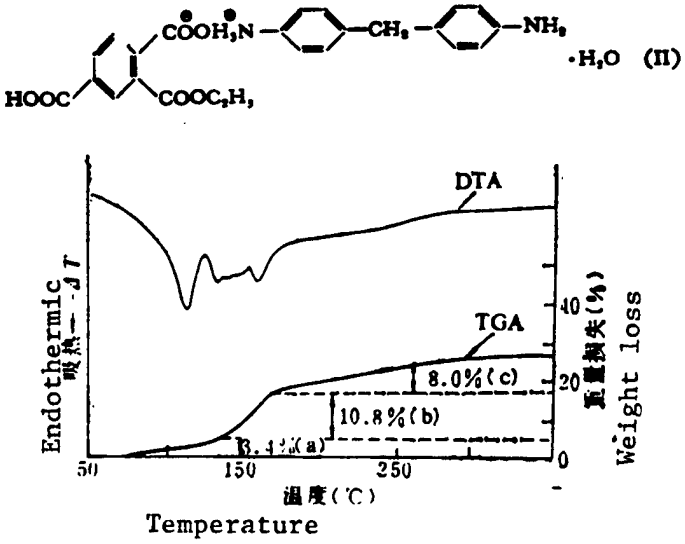

Figure 2. TGA/DTA Traces of Compound II

Therefore, we believe that the amidation reaction probably follows the intramolecular nucleophilic addition-elimination of the carboxylate anion to its neighboring carbonyl group. Because this is a faster reaction than the intramolecular nucleophilic addition in Equation 1 and the endothermic reaction in Equation 2, the amidation can be accomplished within minutes. As to the 3.4 percent (below 140°C) of region a and 8.0 percent (170°-250°C) of region c, they correspond to the loss of one molecule of crystalline water of compound II (3.96 percent) and the sum of the weight loss due to the elimination of water from acid amide to form imide and the weight loss of one molecule of water from 4-carboxylate to form amide bond (7.93 percent).

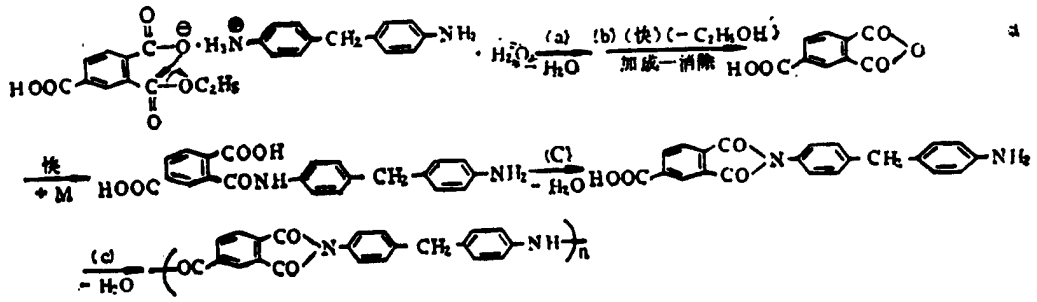

Therefore, it can be seen that, in the "PMR" type PAI, the amidation of 1 and 2 positions occurs through the reaction of the ammonium salt of ester acid. At temperatures beyond the m.p., it follows the fast reaction of ethanol elimination to form anhydride. However, the reaction does not follow the simple intramolecular endothermic mechanism, but rather the intramolecular nucleophilic addition-elimination mechanism between the carboxylate anion and the carbonyl carbon atom.

3. Structure of Low Molecular Weight Polymer

Since the "PMR" type PAI solutions exist as the ammonium salt of ester acid, we carried out a preliminary study of the solid-phase reaction of the resins with n=1 in order to understand, as composite material, the structure of the resin on fabrics after the removal of solvent. The reaction conditions were 120°, 140°, and 160°C for 1 hour. The products were then subjected to liquid chromatography. The results show only the formation of low molecular weight products such as N-M, T-M, T-M-N, and N-M-N. Because no product, N-M-T-M-N, is formed, this agrees with the results of 4-carboxyl amidation of compound T. It can be concluded that for the "PMR" type PAI resins, no large molecule with the structure of N-M-(-T-M-)$_n$-N is produced in the solid-phase reaction at 120°-160°C, whatever the n value. Only such small molecules as N-M, T-M, T-M-N, and N-M-N are generated. The further elongations of the chain and cross-linking reactions occur during the molding process at still higher temperature.

4. Properties

Experimental results show that the formula molecular weight (FMW) of PAI resin has an obvious impact on the breakdown temperature and the flexural strength of the glass cloth-reinforced plastics (Table 2).

N/M/T	FMW	Breakdown temperature (℃)	Flexural strength (kg/cm²)	
			Room temperature	300℃
2/2/1	845	460	5760	4640
2/3/2	1198	478	6290	4640
2/4/3	1552	479	6630	—
2/5/4	1902	488	7070	4430
2/10/9	3676	496	4870	1680
2/20/19	7218	—	4360	1400
0/1/1		500	2040	400

Table 2. Correlation of Formula Molecular Weight with Breakdown Temperature and Flexural Strength

The results also show that FMW also has significant impact on their isothermal aging properties (Figure 3).

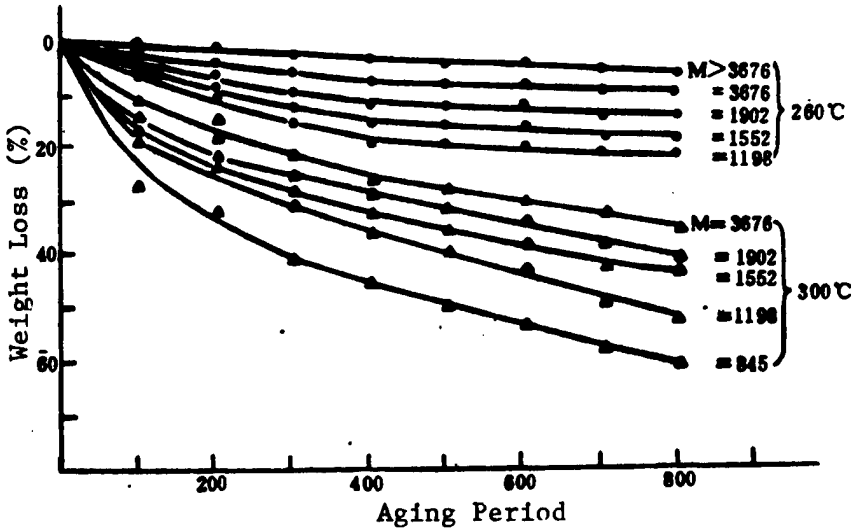

Figure 3. Formula Molecular Weight and Isothermal Aging Behavior

Taking flexural strength and isothermal aging properties into consideration, we believe it is more appropriate to select those PAI with n=3-4 and whose FMW is between 1552-1902.

We ended up choosing a PAI resin with n=3 and FMW=1552 for the fabrication of a glass cloth-reinforced plastic, which was aged for 800 hours at 260°C. The data are shown in Table 3. It can be seen that the flexural strength drops only a little after subjecting to high temperature for 800 hours. Therefore, PAI composites can be used for an extended period of time at 260°C.

1测试温度 (℃)	2 260℃下热老化后的抗弯强度 (kg/cm²)					
	0	100h	200h	400h	600h	800h
3室 温	6300	6020	7080	5440	5230	4450
260℃	4130	4590	4640	4360	4130	3800

Table 3. Flexural Strength of Glass Cloth Reinforced Plastic After Isothermal Aging

Key:
1. Temperature (°C)
2. Flexural Strength After Aging at 260°C
3. Room temperature

In summary, we believe that the "PMR" type PAI resin synthesized in ethanol has the advantages of easy preparation, low cost, and low pressure molding. It is recommended for use as a heat-resistant composite.

Experimental

1. Preparation of Compound I

Trimellitic anhydride (2.84 grams) was dissolved in DMAc (20 ml). A solution of MDA (3.96 grams in 10ml of DMAc) was added dropwise with stirring. The overnight reaction solution was diluted by ethanol (30 ml) and quickly decanted into water (200 ml). The precipitate formed was filtered, washed and dried to get an isomeric mixture of compound I. The neutralization equivalent is 195.0 (Calcd 195.3).

IR spectrum (KBr pellet), cm^{-1}: 3150-3420, broad, (OH, NH); 1705 (carboxylic C=0); 1655 (amide C=0).

Elemental Analysis for $C_{22}H_{18}N_2O_5$: Calcd: C: 67.68; H: 4.65; N: 7.18. Found: C: 67.94, 67.86; H: 4.22, 4.32; N: 7.12, 7.13.

2. Preparation of Compound II

With reference to the method in the document[4]: 1,2,4-trimellitic 2-ethyl ester (m.p. 206 C; neutralization equivalent 119.0, calcd 119.5; chromatographically homogeneous, 11 g) was dissolved in ethanol (45 ml) by heating and quickly poured into a suspension of MDA (9.15 grams) in hot water (30 ml). After complete dissolution by stirring, the solution was kept at 0°C overnight to obtain light yellow solids, which were filtered, washed with petroleum ether-benzene, and dried. The product, compound II, has a m.p. of 111-113°C and a neutralization equivalent of 227.0 (calcd 227.2).

IR spectrum (KBr pellet), cm^{-1}: 3400-3450 (OH, NH); 2600 ($-NH_3$); 1722 (ester C=0); 1705 (carboxylic C=0); 1515 (COO-).

Analysis for $C_{24}H_{24}N_2O_6 \cdot H_2O$: Calcd: C: 63.42; H: 5.77; N: 6.17. Found: C: 63.77, 63.84; H: 5.75, 5.76; N: 5.86, 5.75.

3. Thermal Analysis

Differential thermal analysis (DTA) were done by a Mettler Model TA 2000 DTA instrument. The range was 5 μV and temperature gradient was 10°C/min. Sample size was 2-3 mg. The thermal gravity analysis/differential thermal analysis (TGA/DTA) were recorded on a Model 41 differential thermobalance manufactured by Beijing Optical Instruments Factory. The scales of TGA and DTA were 25 mg and 25 μV, respectively. The temperature gradient was 10°C/min and sample size was 11-12 mg.

4. Preparation of Resin

Compounds N, T, and M were weighed according to a precalculated ratio. Ethanol was added to make a 40-45 percent (w/w) solution of PAI. For example, compounds N (2.80 grams) and T (4.76 grams) were placed in a flask. Ethanol (15.5 grams) was added. After dissolution by heating, compound M (5.28 grams) was added, which was dissolved by stirring to make a 45 percent (w/w) resin solution.

5. Preparation of Reinforced Plastic

Resin solution was applied to the KH 550 pre-treated base-free glass cloth (0.1 mm thick), which was then dried at 80°C. High temperature treatment resulted in a pre-treated fabric. The resin content of the fabric is 30-35 percent. It was then fabricated under a pressure of 10 kg/cm^2 at 300-310°C for 1 hour. The resin content in the final product varies somewhat with molecular weight.

FOOTNOTES

1. Lavin, E., Markhart, A.H., Santer, J.O., USP, 3, 260, 691, 1966.

2. Freeman, J.H., Frost, L.W., Bower, G.M., Traynor, E.J., Burgman, H.A., Ruffing, C.R., POLYM. ENG. SCI., 1969, 9(1), 56-72.

3. Krun, D., Jablenski, R.J., J. POLYM. SCI., POLYM. CHEM. ED., 1979, 17, 1945-51.

4. Wang Dong [3769 2639], Wu Yaoman [0702 3852 2581], Li Jiaze [2621 1367 3149], Zhang Chongli, Yu Shangying [0827 0794 5391], Jin Yirong [6855 6965 3310], and Huang Zhitang, GAOFENZI TONGXUN [POLYMER COMMUNICATIONS], 1980 (3), 152.

12922/7358
CSO: 4008/1099

SYNTHESIS OF POLYBUTADIENE BY NEW CATALYST SYSTEM STUDIED

Beijing GAOFENZI TONGXUN [POLYMER COMMUNICATIONS] in Chinese No 3, Jun 86 pp 236-240

[Article by Xu Ling [1776 3781], Zhao Senkun [6392 2773 2492], and Tang Xueming [0781 1331 2494], Qingdao College of Chemical Technology; Paper received 17 February 1985; Research financed by Science Fund administered by Chinese Academy of Sciences]

[Text] In the previous paper,[1] we reported the synthesis of polybutadiene by the catalyst system $MoCl_n(OC_8H_{17})_{4-n}$-(i-Bu)2AlOPh. It is observed[2] that $MoCl_n(OC_8H_{17})_{4-n}$ dissolves better than $MoCl_4$ in hydrogenated gasoline and displays better catalytic activity. Based on these previous works, we investigated in this paper the correlation of the solubility of $MoCl_n(OR)_{4-n}$ in hydrogenated gasoline and their catalytic behavior with the functional group R by choosing different OR groups. We studied the effect of the dosage and ratio of main catalyst and cocatalyst on the catalysis of polymerization, polymer mean molecular weight, and molecular weight distribution. The microscopic structure of large polymers were studied by IR spectroscopy.

Purifications of butadiene (Bd) and hydrogenated gasoline and the preparation of catalyst and condition of polymerization are as described.[1]

The polymer molecular weight distributions were determined in THF by a Model NJ-762 gel permeation chromatograph. The microscopic structures were determined by IR spectroscopy (Shimadzu model IR-408) following the literature procedure.[3]

1. Solubility of $MoCl_n(OR)_{4-n}$

Various alkyl, cycloalkyl, and benzyl alcohols and phenols with R ranging from C1-10 were chosen to react with $MoCl_4$. The results show that the reaction goes faster with a smaller R. The products from those with an alkyl group of less than four carbons are insoluble in hydrogenated gasoline. The product with isobutyl group has better solubility than that with n-butyl group and those with an alkyl group of more than five carbons have good solubility. When R is cycloalkyl, benzyl, or phenyl, their products dissolve poorly. In the reactions of cyclohexyl alcohol and benzyl alcohol with $MoCl_4$, a small amount of ethyl acetate was added. The solubility and catalytic activity were improved in the former and there was very little difference in the latter.

The results show that temperature also affects the solubility. Higher temperature results in higher solubility. White precipitates appear when dissolving $MoCl_n(OC_{16}H_{33})_{4-n}$ at room temperature which can be redissolved by applying heat.

2. Correlation Between the Catalytic Activity of $MoCl_4(OR)_{4-n}$ and the R Group

Soluble $MoCl_n(OR)_{4-n}$ (abbreviated as Mo) as a main catalyst and $(i\text{-}Bu)_2AlOPh$ (abbreviated as Al) as a co-catalyst were used to catalyze the polymerization of butadiene. The results show that for all R groups, the conversion rate reaches a maximum at a certain Al/Mo value (molar ratio), which varies with R (see Figures 1 and 2).

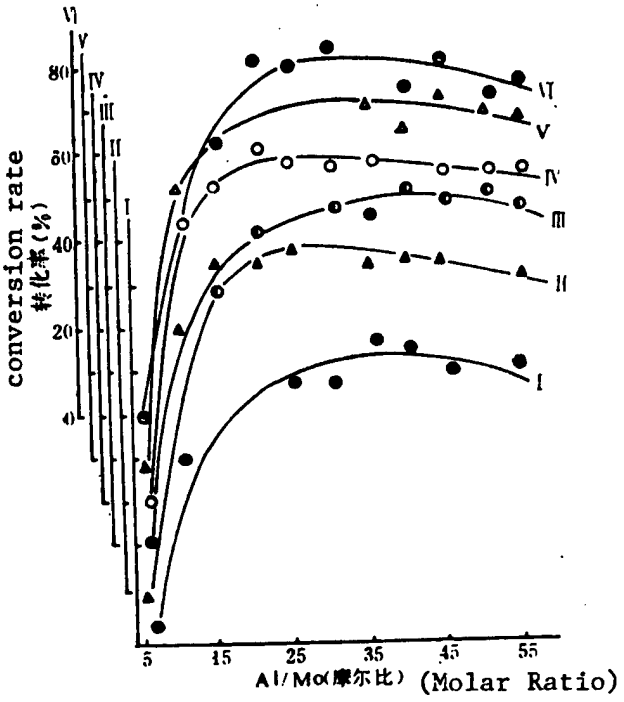

I. $MoCl_n(OC_4H_9)_{4-n}$; II. $MoCl_n(OC_5H_{11})_{4-n}$
III. $MoCl_n(OC_8H_{17})_{4-n}$; IV. $MoCl_n(OC_9H_{19})_{4-n}$
V. $MoCl_n(OC_{10}H_{21})_{4-n}$; VI. $MoCl_n(OC_{16}H_{33})_{4-n}$
ROH/Mo = 8; Mo/Bd = 2.0×10^{-4}; 50℃;
7小时
hours

Figure 1. Effect of Al/Mo Ratio on Conversion Rate

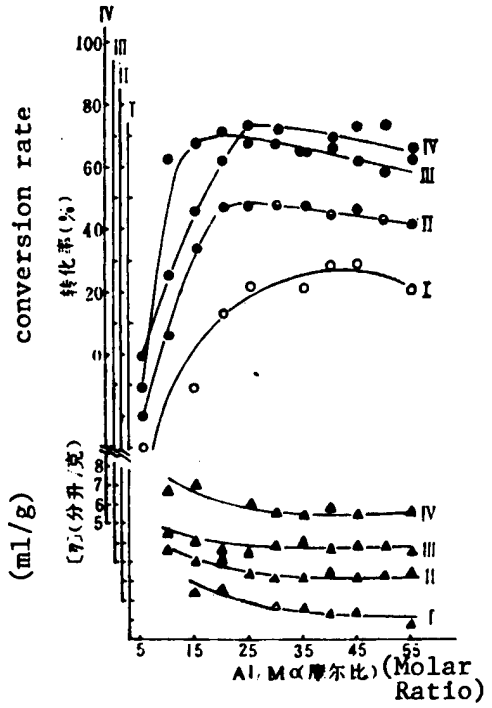

I. $MoCl_n(t\text{-}OC_7H_{15})_{4-n}$;
II. $MoCl_n(S\text{-}OC_8H_{11})_{4-n}$
III. $MoCl_n(i\text{-}OC_5H_{11})_{4-n}$;
IV. $MoCl_n(i\text{-}OC_4H_9)_{4-n}$

Figure 2. Effect of Al/Mo Ratio on Conversion Rate and Inherent Viscosity

It can be seen from Figures 1 and 2 that the catalytic activity of $MoCl_n(t\text{-}OC_7H_{15})_{4-n}$ is lowest and that of $MoCl_n(s\text{-}OC_5H_{11})_{4-n}$ is next to lowest. The $MoCl_n(OR)_{4-n}$ has a level of higher activity when the R is n-alkyl or i-alkyl. Thus, the order of activity is primary > secondary > tertiary alcohol. What is different from the pentavalent Mo system[4] is that i-alkyl R group gives better activity than n-alkyl group does in this system and that whether the carbon number of R group is odd or even has no effect on the solubility and catalytic activity. The conversion rates for all R groups are better than that with the Mo(V) system alone. It takes a smaller amount of Al than Mo(V) to achieve the same conversion rate. The Al/Mo value range that is appropriate for this system is broad.

The R group has little effect on the polymer mean molecular weight and molecular weight distribution (see Figures 2 and 3 and Table 1).

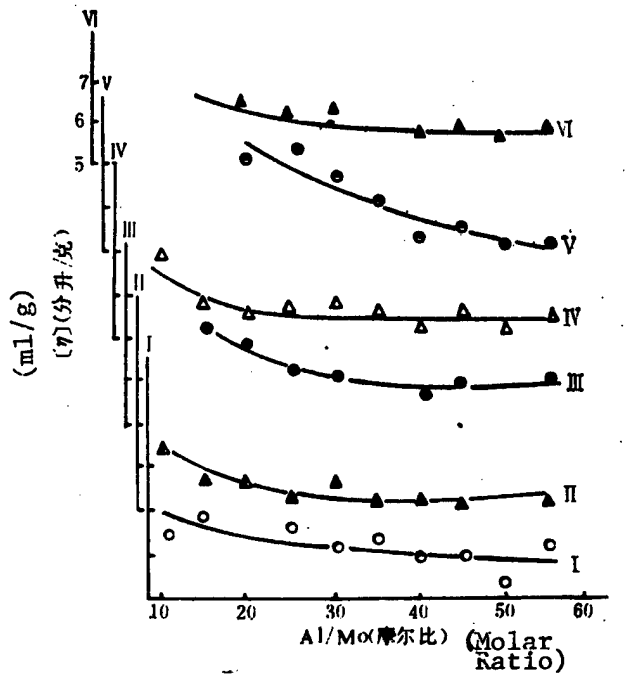

Figure 3. Effect of Al/Mo Ratio on Inherent Viscosity

R Group	Al/Mo* (Molar Ratio)	$\bar{M}_w \times 10^{-4}$	$\bar{M}_n \times 10^{-4}$	$\bar{M}_w/\bar{M}_n$
n-C_4H_9	35	1.83	5.9	3.09
i-C_4H_9	25	1.86	6.9	2.69
n-C_5H_{11}	30	1.81	4.7	3.81
i-C_5H_{11}	20	1.57	5.3	2.97
t-C_7H_{15}	40	1.94	6.9	2.79
n-C_8H_{17}	50	1.75	5.7	3.10
n-C_9H_{19}	20	1.48	4.6	3.19
n-$C_{10}H_{21}$	45	1.69	6.2	2.69
n-$C_{16}H_{33}$	30	1.86	6.4	2.94

* The Al/Mo value for maximum conversion; Mo/Bd = 2.0×10^{-4}

Table 1. Effect of R Group on Molecular Weight Distribution

It can be seen from Figures 2 and 3 that Al/Mo also has little effect on the polymer mean molecular weight. The [η] decreases slightly with an increase in the Al/Mo value when the latter is small. After the Al/Mo value reaches 30, [η] is basically constant. This suggests that there is less chain transfer toward Al in this system.

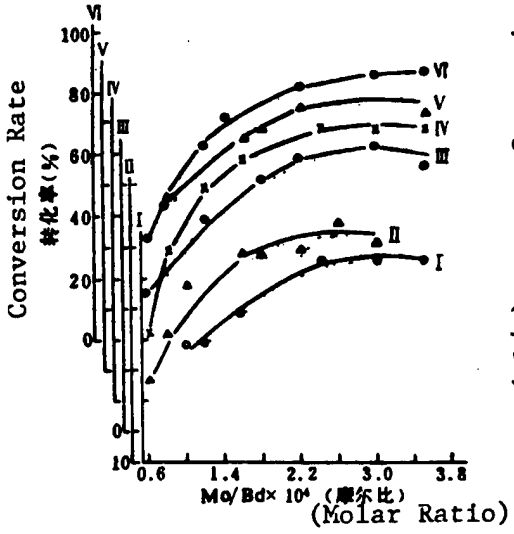

Al/Bd = 4.0×10^{-3}
(see Figure 1 for details.)

Figure 4. Effect of Mo Dosage on Catalytic Activity

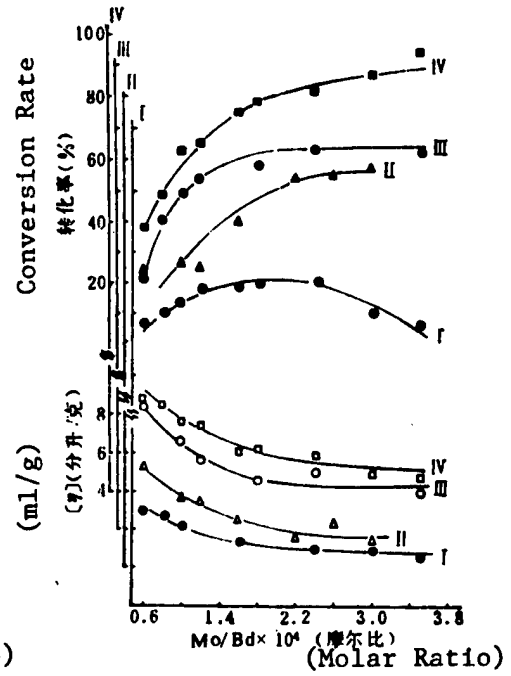

(see Figure 2 for details.)

Figure 5. Effect of Mo Dosage on Conversion Rate and Inherent Viscosity

3. Dosage and Catalytic Activity of $MoCl_n(OR)_{4-n}$

It can be seen from Figure 4 that the conversion rate increases with an increasing Mo dosage regardless of the R group. When R are n-alkyls, the conversion rates all reach over 80 percent at the Mo/Bd ratio of 2.0×10^{-4} (molar ratio). The catalytic activity increases slightly with the increasing R group.

Figure 5 shows the catalytic activities of several catalysts with the branched R group. It can be seen that the catalytic activities of primary, secondary, and tertiary alcohol-substituted $MoCl_n(OR)_{4-n}$ are different. This is consistent with the results in Figures 1 and 2.

The Mo dosage has a greater effect on molecular weight. [η] decreases with the increasing Mo/Bd (see Figures 5 and 6). When R is n-alkyl, [η] value is slightly smaller.

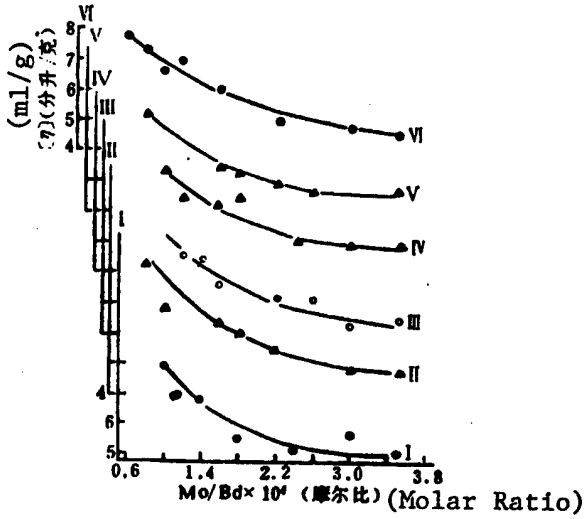

(See Figure 1 for details.)

Figure 6. Effect of Mo Dosage on Inherent Viscosity

4. Microscopic Structures of the Polymers

The microscopic structures of the polymers with different R groups are listed in Table 2. It can be seen that changes in the R group have little effect on the microscopic structure. There are almost no 1,4-trans linkage and about 10 percent of 1,4-cis linkages. The content of the 1,2-linkage is constant, over 80 percent.

R Group	Al/Mo* (Molar Ratio)	Microscopic structure (%)		
		trans 1,4-	1,2-	cis 1,4-
$n\text{-}C_4H_9$	35	0	91	9
$i\text{-}C_4H_9$	25	0	89	11
$n\text{-}C_5H_{11}$	30	0	88	12
$i\text{-}C_5H_{11}$	20	1	82	17
$s\text{-}C_5H_{11}$	25	1	88	11
$t\text{-}C_7H_{15}$	40	0	91	9
$n\text{-}C_8H_{17}$	50	0	90	10
$n\text{-}C_9H_{19}$	20	0	93	7
$n\text{-}C_{10}H_{21}$	45	0	91	9
$n\text{-}C_{16}H_{33}$	30	1	90	9

* The Al/Mo ratio for maximum conversion.

Table 2. Effect of R group on Microscopic Structure

FOOTNOTES

1. Xu Ling, Yan Chunzhen [7051 2504 3791], and Tang Xueming, HECHENG XIANGJIAO GONGYE [SYNTHETIC RUBBER INDUSTRY], 1985, 1, 21.

2. Yan Chunzhen and Tang Xueming, "The Collected Papers of Changchun Institute of Applied Chemistry," Chinese Academy of Sciences, 1982, 2, 56.

3. Zeng Huanting [2582 3562 1656], HECHENG XIANGJIAO GONGYE [SYNTHETIC RUBBER INDUSTRY], 1978, 2, 56.

4. Ni Shaoru [0242 1421 0320] and Tang Xueming, HECHENG XIANGJIAO GONGYE [SYNTHETIC RUBBER INDUSTRY], 1982, 5, 444.

12922/7358
CSO: 4008/1099

DDC-ENHANCED KILLING EFFECT OF HPD-LASER ON TUMOR CELLS

Shanghai ZIRAN ZAZHI [NATURE JOURNAL] in Chinese Vol 9, No 5, May 86 pp 395-396

[Article by Mo Jian [5459 4675], Wang Duoning [3769 1122 1337], Sun Shufen [1327 3219 5358], Li Aiqun [2621 1947 5028], Luo Wenbo [7482 2429 0590], Guo Youchi [6753 0645 3069], and Liu Yaohua [0491 1031 5478], PLA Fourth Military Medical College; paper received 20 May 1985]

[Text] The treatment of tumors by the combination of hematoporphyrine derivative (HPD) and a laser has shown promising clinical results. Its mechanism may involve damaging the cancer cells by reactive oxygen ($^1O_2$) and lipid peroxidation. We suggested that its therapeutic effect could be raised if the cancer cells' ability to withstand the damage of reactive oxygen species and lipid peroxidation is reduced.[1, 2] DDC (sodium diethylaminodithiocarboxylate) inhibits the activity of superoxide dismutase and glutathione peroxidase,[3] which in turn reduces the ability of cancer cells to withstand the damage caused by reactive oxygen species and lipid peroxidation. Therefore, we carried out the DDC-HPD-laser experiments on cancer cells. Five different experiments were done in 3.5-cm (inner diameter) weighing bottles. Each contained $2x10^6$ Ascites tumor cells, 1 ml of 10 percent calf serum-RPMI 1640 medium (pH 7.4), and other ingredients (see Table 1). The concentration of DDC was $1.5x10^{-2}$M when present. There were kept at 37°C immediately after the DDC addition. HPD, 10 ul of a 5-mg/ml solution (manufactured by the Beijing Institute of the Pharmaceutical Industry), was added 4.5 hours later. Laser irradiation was then carried out 1.5 hours after the addition of HPD. The laser output power is 7mW (He-Ne laser model ZN-450, Xingping Radio Factory). Samples were placed 86.5 cm from the source and the laser light was dispersed into a spot of 3.8 cm in diameter. The irradiation time was 10 minutes. The viable cells, determined by their exclusion of Trypan Blue, were counted 1, 3, and 5 hours after irradiation. Each experiment was repeated 12 times and the results were shown in Table 1.

It can be seen from the cell counts after 5 hours that the HPD-laser combination has an obvious killing effect on cancer cells, the cell death rate being raised from 6.7 to 31.2 percent. DDC shows a clear enhancement of the effect and further raises the death rate from 31.2 to 100 percent ($P < 0.01$). The results of cell counts after 3 hours are as follows: in experiment 1, where DDC, HPD, and a laser were used together, the death rate of cancer cell reached 92.9 percent; in experiments 2, 3, and 4, when DDC, HPD, or a laser was

omitted, the death rates were below 30 percent and the sum of any two of them was still far lower than that of experiment 1. This shows that DDC, HPD, and a laser contribute synergistically to the killing of cancer cells.

Experiment No.	Death percentage ($\bar{X}$±SD)		
	1hr	3 hr	5hr
I. DDC+HPD+Laser	89.1± 9.8	92.9± 5.2	100± 0
II. HPD+ Laser	10.6± 7.1	15.9± 15.8	31.2± 9.3
III. DDC+ Laser	25.1± 10.6	25.2± 21.2	
IV. DDC+HPD	21.3± 11.6	28.2± 16.7	
V. Control	6.5± 4.4	5.8± 6.9	6.7± 4.8

Table 1. Killing Effect of HPD-laser on Cancer Cells and Enhancement by DDC

Use of the DDC-HPD-laser approach to treat tumors in animal is currently underway. Preliminary results show that DDC also enhanced the therapeutic effect of HPD-laser under certain conditions.

FOOTNOTES

1. Mo, Jian, "Progresses in Biochemistry and Biophysics," 5, (1984) 11.

2. Nathan, C.F., FED. PROC., 41 (1981) 2206.

3. Smith, M.J., et al., BIOCHEM. PHARMACOL., 31 (1982) 19.

12922/7358
CSO: 4008/1084

EVOLUTION SITES IN RIBOSOMAL 5S RNA STRUCTURE

Shanghai ZIRAN ZAZHI [NATURE JOURNAL] in Chinese Vol 9, No 5, May 86 pp 396-397

[Article by Qi Guorong [4359 0948 2837], Cao Gongjie [2580 0501 2638], Jiang Peng [3068 7720], Feng Xiaoli [7458 2556 7812], and Gu Xiangrong [6581 4382 2837], Shanghai Biological Chemistry Institute, Chinese Academy of Sciences; paper received 18 October 1985]

[Text] The earliest studies of evolution and developmental biology at the molecular level were done on protein molecules such as hemoglobin and cytochrome C. In recent years, there is a widespread use of small pieces of nucleic acid to study the evolution of molecules. 5S rRNA exists in all forms of life and is the direct product of gene expression. Its biological functions do not vary among species. Thanks to the revolutionary breakthrough in DNA sequence analysis methodologies and the fact that 5S rRNA does not contain modified bases, the primary structure of over 250 5S rRNA's has been determined by 1984.[1] This makes it even more appropriate to study biological evolution through the structure of 5S rRNA. Osawa and Hori have established a molecular evolution tree model for 5S rRNA[2] through comparisons of the base compositions of various 5S rRNA's. But they have not examined the correlation between base change in each position of the 5S rRNA and evolution.

Since 1979, we have determined the primary structure of six 5S rRNA's from different sources, including the highest invertebrate lancelet (branchiostoma belcheri, subphylum cephalochordata), the lowest vertebrate lamprey (lampetra reissneri, subphylum vertebrata, class cyclostomata), three kinds of silkworm (castor silkworm,[3] tussah, and hybride), and cottonseed.[4] We compared our results with the published sequences of eucaryotic 5S rRNA's[1] and observed some significant phenomena. Comparisons were made at the secondary structure level. Using the generally accepted secondary structure model of De Wachter, et al.,[5] we examined the structural features of over 170 eucaryotic 5S rRNA's and made the graphic presentations of their structures. As shown in Figure 1, there are four kinds of sites in the structure: (1) conserved, (2) semi-conserved, (3) random mutation, and (4) evolution. We find that these evolution sites within the 5S rRNA structure are closely related to biological evolution. This discovery provides further insight into the study of molecular evolution. Take, for example, the animal kingdom. In the evolution of species, there are sequential changes in these evolution sites. Some of them occur at the early stage of the evolution and others later. Once the change takes place,

it is conserved throughout the subsequent evolutions (Table 1). If more sequences of 5S rRNA are determined, particularly those of the species that occupy unique places in the evolution, the results in the table can be expected to be improved and the classification of these sites further refined. Though we do not understand the cause and biological significance of these "ordered" changes, at least the phenomenon can be used as a marker, i.e., the classification of a species and its place in the evolution can be determined from the primary structure of its 5S rRNA by following the rules of evolution site we proposed.

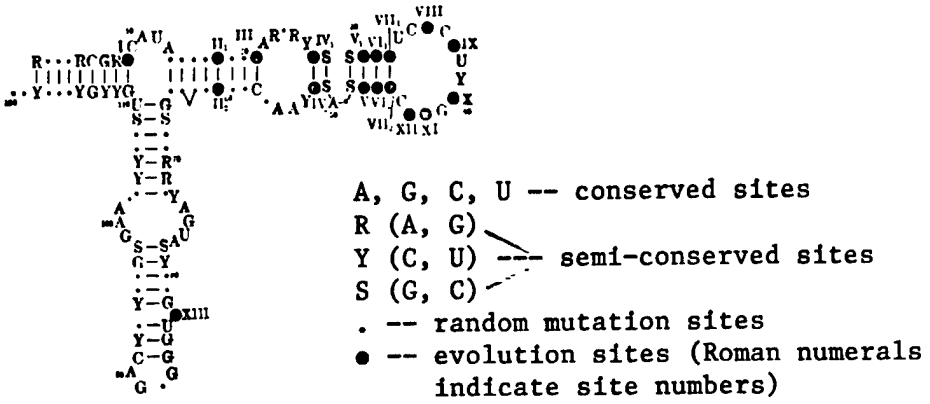

Figure 1. Structural Features of Eucaryotic 5S rRNA's

Evolution site #			I	II	III	IV_1-IV_3	V	VI	VII	VIII	IX_1-IX_3	X_1-X_3	XI_1-XI_3	XII_1-XII_3	XIII
Base position #			9	42	21	31—46	35	83	43	37	30—47	18—60	27—52	40	
Protozoa			C	C	U,A	C-G	C	G	A	A	G-C	G-C	A-U	C	
				A	G	G-C			U	G					
Parazoa			C	A	G	G-C	U	C	C	A	C-G	G-C	A-U	C	
Metazoa	Other vertebrates (porifera→ Echinoderms)		C	A	G	G-C	U	A	U	G	G-C	G-C	A-U	C	
	Protochordate	Hemichordate	C	A	G	G-C	U	A	U	G	G-C	G-C	A-U	C	
		Tunicate	C	A	G	G-C	U	A	U	G	C-G	A-U	A-U	C	
		Cephalochordate	C	A	G	G-C	U	A	U	G	C-G	G-C	A-U	C	
	Vertebrate	Class cyclostomata	C	A	G	G-C	U	A	U	G	C-G	C-G	G-C	C	
		Class Osteichthyes	C	A	G	G-C	U	A	U	G	C-G	C-G	G-C	C/U	
		Class Amphibia→Class Maxmalia	C	A	G	G-C	U	A	U	G	C-G	C-G	G-C	U	

Table 1. Evolution Sites in Animal 5S rRNAs

* Only those occurring over 90 percent of the time are included.

FOOTNOTES

1. Erdmann, V.A., et al., NUCL. ACIDS RES., 13 (1985), suppl. r105.

2. Osawa, S., and Hori, H., "Ribosomes--Structure, Function, and Genetics," Chambliss, G., et al., eds., University Park Press, Baltimore (1980) p 333.

3. Cao, Gongjie, et al., SHENGWU HUAXUE YU SHENGWU WULI XUEBAO [JOURNAL OF BIOCHEMISTRY AND BIOPHYSICS], 15, 5 (1983) p 406.

4. Qi, Guorong, et al., ZHONGSHAN DAXUE XUE BAO (ZIRAN KEXUE BAN) [JOURNAL OF ZHONGSHAN UNIVERSITY (NATURAL SCIENCES EDITION)], 2 (1985) p 65.

5. De Wachter, et al., BIOCHEM., 64 (1982) p 311.

12922/7358
CSO: 4008/1084

SYNTHESIS OF POLYNUCLEOTIDES BY PNPase STUDIED

Shanghai ZIRAN ZAZHI [NATURE JOURNAL] in Chinese Vol 9, No 5, May 86 p 398

[Article by Wang Qisong [3769 0796 2646] and Shang Jinbao [0794 6855 1405], Shanghai Biochemistry Institute, Chinese Academy of Sciences, and Dai Dingming [2071 1353 2494], Shanghai Chemical Reagents Plant No 2; paper received 26 April 1985]

[Text] The authors have reported the 3'-end phosphorylation of oligonucleotides by polynucleotide phosphatase (PNPase).[1] In this article, the method is applied to the synthesis of polynucleotides. The principle is that nucleoside diphosphate and 7-methyl guanosine diphosphates (^{m7}GDP) are polymerized by PNPase in the presence of a premier. The 7-methyl guanine residues in the polymer are then selectively removed. In this fashion, a limited number of nucleotides can be introduced at the 3'-end of the primer. The number of nucleotides introduced can be controlled by the ratio of nucleoside diphosphates and ^{m7}GDP. For example, we used 120 O.D. (A260) of the trinucleotide CpUpC as a primer and reacted them with 16 mg of GDP and 8 mg of ^{m7}GDP in the presence of PNPase. The ^{m7}G residues in the polymer were then selectively removed.[1] The resulting products CpUpCpGp, CpUpCpGpGp, and CpUpCpGpGpGp were separated by DEAE-Sephadex A25 column chromatography. The chromatogram is shown in Figure 1. Peaks III, V, VII, and VIII are homogeneous with both solvent systems I and II. Peak III is identified as CpUpCp and peak V CpUpCpGp by comparison with the standards. Peaks VII and VIII are identified as CpUpCpGpGp and CpUpCpGpGpGp, respectively, by spectral measurement and base composition determination after calf pancreatic ribonuclease digest. Peaks IV and VI are heterogeneous. Their spectra show the peaks of guanylic acid and are possibly the oligo(G)'s from the hydrolysis of the polymer CpUpCp(Gp)n-(^{m7}Gp)m. Such data as the spectral radio, Rf value, base composition, and yields for peaks III, V, and VII are listed in Table 1.

When the ratio was changed to GDP:^{m7}GDP = 3:1, the result was the increased yield of longer chains CpUpCp(Gp)n($n > 4.5$) while the yields of CpUpCp and CpUpCpGp were lowered. When using $^{m'}$IpΨ and Cp$^{m'}$Ψ as a primer to copolymerize with a certain ratio of GDP and ^{m7}GDP, results similar to the chromatogram shown in Figure 1 were obtained, suggesting the general applicability of the method. This method is particularly suitable for synthesizing those oligonucleotides with stretches of a particular base, a common occurrence in mRNA, 5S rRNA, and tRNA.

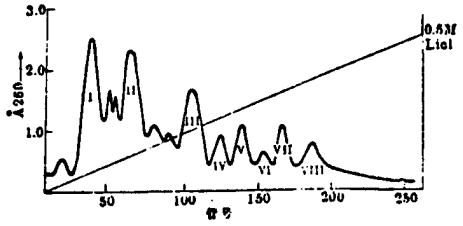

Figure 1. Column Chromatography Profile of CpUpCp(Gp)n

Column: DEAE-Sephadex A25 HCO_3 type (1x30 cm).
Initial eluant: 0.02M Tris·HCl (pH 7.2), 7M urea.
Final gredient: 0.02M Tris·HCl (pH 7.2), 7M urea, 0.5M LiCl.
Flow rate: 5 ml/15 min; 5 ml/tube.

a 样品	光谱比值 b A_{250}/A_{260}		光谱比值 b A_{280}/A_{260}		R_f 值		d 碱基组成	产率 e (%)
	pH2	pH7	pH2	pH7	溶剂 I c	溶剂 II c	U_p:C_p:G_p	
峰 II	0.66	0.90	1.09	0.69	0.97*	0.94*	1.0:2.1 :0	~30
f 峰 V	0.77	1.03	0.91	0.70	0.97**	0.99**	1.0:2.07:1.02	13~16
峰 VI	0.84	1.02	0.89	0.70	0.50*	0.09*	1.0:1.98:2.1	~9
峰 VII	0.93	1.01	0.85	0.71	0.22*	0.05*	1.0:2.05:2.9	~5

Key:
a. sample
b. spectral ratio
c. solvent system
d. base composition
e. yield
f. peak

Table 1. Spectral Ratio, Rf Value, Base Composition and Yield of Samples

* The Rf of the standard CpUpCp = 1.
** The Rf of the standard CpUpCpGp = 1.
Solvent I: 95% ethanol : 1 M ammonium acetate = 6 : 5 (v/v)
Solvent II: 2-butanoic acid : 1M ammonium hydroxide : 0.1M EDTA = 100 : 60 : 0.6 (v/v).

FOOTNOTES

1. Wang, Qisong, SHENGWU HUAXUE YU SHENGWU WULI XUEBAO [JOURNAL OF BIOCHEMISTRY AND BIOPHYSICS], 11, 3 (1979) p 207.

12922/7358
CSO: 4008/1084

INVESTIGATION OF STIMULATED BRILLOUIN SCATTERING SPECTRA IN LASER-PLASMA INTERACTIONS

Shanghai ZHONGGUO JIGUANG [CHINESE JOURNAL OF LASERS] in Chinese Vol 13 No 8, 20 Aug 86 pp 449-456, 461

[English abstract of article by Tang Yonghong [0781 3057 4767] and Xu Zhizhan [1776 5267 1455] of Shanghai Institute of Optics and Fine Mechanics, Chinese Academy of Sciences]

[Text] Equations describing Brillouin backscattering are obtained in one-dimensional inhomogeneous plasma. Based on the equations, the scattering spectra are calculated both for linear and nonlinear multimode instability. For a thermal noise source, the spectral shape is dependent on the ion-acoustic wave damping, the plasma inhomogeneity and the incident light depletion. The resultant spectra, including these effects, are in agreement with experimental observations.

LASER PULSE COMPRESSION AND AMPLIFICATION BY STIMULATED BRILLOUIN SCATTERING

Shanghai ZHONGGUO JIGUANG [CHINESE JOURNAL OF LASERS] in Chinese Vol 13 No 8, 20 Aug 86 pp 457-461

[English abstract of article by Yang Jingguo [2799 4842 0948], et al., of the Department of Physics, Sichuan University]

[Text] A 30 ns ruby laser pulse is compressed to about 6 ns with acetone (C_3H_6O) by SBS. The Stokes pulse is then amplified again in a laser amplifier, with the energy gain being greater than 5 and the total power gain about 60. The characteristics and applications of the technique are discussed.

TUNABLE LASER SOURCE AT WAVELENGTH DOWN TO 218.3 NM

Shanghai ZHONGGUO JIGUANG [CHINESE JOURNAL OF LASERS] in Chinese Vol 13 No 8, 20 Aug 86 pp 466-469

[English abstract of article by Yang Xiangchun [2799 7449 2504] and Zhang Xinnan [1728 2450 8189], et al., of Shanghai Institute of Optics and Fine Mechanics, Chinese Academy of Sciences]

[Text] Calculation results of frequency doubling and frequency summing phase matching parameters for different wavelengths using KDP-type crystals are given. Experimental verification has been performed, nad a tunable wavelength down to 218.3 nm has been obtained.

SECOND HARMONIC GENERATION WITH UREA CRYSTAL BY Ar^+ LASER LIGHT

Shanghai ZHONGGUO JIGUANG [CHINESE JOURNAL OF LASERS] in Chinese Vol 13 No 8, 20 Aug 86 pp 478-481

[English abstract of article by Zeng Yongjian [2582 3057 0256], et al., of Shanghai Institute of Laser Technology; Su Genbuo [5685 2704 0590], et al., of Fujian Institute of Material Structure]

[Text] Characteristics of the second harmonic generation at three lines, 514.5, 496.5 and 488.0 nm, with a urea crystal by Ar^+ laser light is reported in detail for the first time. The phase mismatch at the azimuthal angle due to the thermal effect has been found. The dependence of frequency-doubling efficiency upon other parameters is given.

OUTPUT AND MEASUREMENT OF RADIATION IN FREE-ELECTRON LASER BASED ON STIMULATED RAMAN SCATTERING

Shanghai ZHONGGUO JIGUANG [CHINESE JOURNAL OF LASERS] in Chinese Vol 13 No 8, 20 Aug 86 pp 482-484, 481

[English abstract of article by Chu Cheng [5969 2052], et al., of Shanghai Institute of Optics and Fine Mechanics, Chinese Academy of Sciences]

[Text] The authors have succeeded in obtaining laser action in a free-electron laser based on stimulated Raman scattering. This paper presents a brief account of the output and measurement of the free-electron laser radiation in the Ka band. The design method of the drift tube, emitting and receiving horns and filters are summarized together with radiation measurement results.

LASER HETERODYNE BIAS FREQUENCY-LOCKING FOR COHERENT OPTICAL COMMUNICATION

Shanghai ZHONGGUO JIGUANG [CHINESE JOURNAL OF LASERS] in Chinese Vol 13 No 8, 20 Aug 86 pp 489-492

[English abstract of article by Liao Shiqiang [1675 0013 1730], et al., of Shanghai Institute of Optics and Fine Mechanics, Chinese Academy of Sciences]

[Text] A new frequency modulation system for lasers by heterodyne bias frequency-locking is proposed and developed. The technique can be used in heterodyne or coherent single mode optical communication. Experiments on the grating-tuned CO_2 laser system and Zeeman He-Ne laser system are described. A radio broadcast has been relayed successfully in the locked system. The conditions for practical optical fiber communication with a semiconductor laser and the heterodyne bias frequency-locked system are discussed.

9717
CSO: 4009/112

NOVEL DEFECT IN LEC In-DOPED GaAs SINGLE CRYSTALS

Beijing BANDAOTI XUEBAO [CHINESE JOURNAL OF SEMICONDUCTORS] in Chinese
Vol 7 No 4, Jul 86 pp 341-345

[English abstract of article by He Hui [0149 2547], et al., of the Institute of Semiconductors, Chinese Academy of Sciences]

[Text] A novel defect has been found in LEC In-doped GaAs single crystals. It is a rectangular area in which longer edges are parallel to one of two <110> directions and have a high density of dislocations. Its In content is higher than that of the matrix. Its crystallographic and chemical properties have been studied by SEM-CL, EPMA, CTEM, HREM and XRT techniques. A possible explanation for its origin is suggested, i.e., the formation of this defect is related to the cellular growth under composition supercooling, and it is inherent in continuous solid solution systems, such as $In_xGa_{1-x}As$. (Paper received 5 September 1985.)

REFERENCES

[1] Masamichi Ohmori, "Gallium Arsenide Integrated Circuits", 11th. Int. Symp. on GaAs and Related Compounds, Biarritz, 1984.
[2] M. Duseaux and S. Martin, "Growth and Characterization of Large Dislocation-Free GaAs Crystals for Integrated Circuits Appilations", 3rd Conf. on Semi-Insulating III-V Materials, pp. 118—125 (1984).
[3] H. M. Hobgood, *et al.*, "Large Diameter, Low Dislocation In-Doped GaAs: Growth, Characterization and Implications for FET Fabrication", *ibid.*, pp. 149—156 (1984).
[4] 林兰英等,"低位错密度的 LEC-SI-GaAs 单晶", 砷化镓及有关化合物会议, 峨眉, 1985.
[5] 冈乃本, "晶体生长的物理基础", 第五章第二节 (1982).

LOW DOSE B^+ AND P^+ IMPLANTATION ASSOCIATED DEFECTS IN n-Si AND THEIR ANNEALING BEHAVIORS

Beijing BANDAOTI XUEBAO [CHINESE JOURNAL OF SEMICONDUCTORS] in Chinese
Vol 7 No 4, Jul 86 pp 363-373

[English abstract of article by Chen Jianxin [7115 1696 2450], et al., of the Graduate School, University of Science and Technology of China]

[Text] Detailed information of hole (H) as well as electron (E) traps produced by low dose (10^{11} cm^{-2}) B^+ and P^+ ion implantation in n-Si and their annealing behavior is reported. The hole traps are investigated for the first time. For B^+ implantation, five hole traps are produced: two B related acceptor levels, $H_2(0.62)$, $H_3(0.49)$, of huge concentrations, and three other hole traps, $H_4(0.37)$, $H_1(0.63)$, $H_5(0.15)$. H_4 is probably a C related acceptor. For P^+ implantation, four hole traps are produced: H_2" (0.15) of huge concentration, and $H_4(0.37)$, $H_1(0.63)$, H_5". Electron traps are also reported. For B^+ implantation, seven electron traps are produced: B related acceptor $E_3(0.35)$ with huge concentration at 280°C annealing temperature (AT), E_6, E_7 with small concentrations and shallow levels which are hard to test precisely, but they anneal out drastically above 320°C. The other three E traps, $E_2(0.41)$, $E_4(0.25)$ and $E_5(0.15)$, are detected in both B^+ and P^+ implantation, and are consistent with previous reports for ion, neutron and electron irradiation induced defects of V_{2-} (P.V), $V_{2-}{}^6$, and (O.V) centers respectively. Another low concentration, $E_1(0.45)$, is also detected for B^+ implantation. Annealing behavior of E and H traps are reported. At 800° AT, all traps diminish to average concentrations of less than 10^{12} cm^{-3}. (Paper received 9 May 1985.)

REFERENCES

[1] 北京师范大学: "离子注入原理与技术", 北京出版社, 1982.
[2] 罗晋生: "离子注入物理", 国防工业出版社, 1980.
[3] L. C. Kimerling and J. M. Poate: Defect and Radiation effects In semiconductors, 1974 (Inst. Phys. Conf. Ser. no. 23. London, 1975) p. 126.
[4] K. Masuda, Radiation effects In Semiconductors. 1976. Ed. N. B. Urli and J. W. Corbett (Inst. Phys. Conf Ser. no. 31. London, 1977) p. 174.
[5] J. R. Troxell, *Solid State Electronics*, 26, 539(1983).
[6] J. W. Corbett and J. C. Bourgoin, Point Defects in Solids, Vol. 2, Ed, J. H. Crawford Jr and L. M. Slifkin (Plenum, New York, 1975) p. 1.
[7] J. W. Corbett *et al.*, Radiation effects in semiconductors 1976, Ed. n. b. urli and J. W. Corbett. (Inst. Phys. Conf. Ser. no. 31, London, 1977) p. 174.
[8] W. M. Penney, L. Lau, Mos integrated circuits, (Van Nostrand, New York, 1972).
[9] G. G. Qin (秦国刚), M. F. Li (李名复) and C. T. Sah, *J. Appl. Phys.*, 53, 4800(1982).
[10] D. V. Lang, *J. Appl. Phys.*, 45, 3023(1974).
[11] A. Wang and C. T. Sah, *J. Appl. Phys.*, 56, 1021(1984).
[12] S. M. Sze. Physics of semiconductor de vices, (Wiley, New York, 1969)
[13] O. Engstrom and A. Alm, *Solid State Electronics*, 21, 1571(1978).
J. E. Lowther, *J. Phys. C. Solid State Phys.*, 13, 3681(1980).
秦国刚, 姚秀琛, 中国科学, A(1984) No.5, 432
[14] J. M. Meese, Defects in Semiconductors, Ed.J. Naravan and T. Y. Tan. (North Holland. New York, 1981), p. 225.
[15] 杜永昌、张玉峰、秦国刚, 半导体学报, 5, 7(1984),
[16] L. C. Kimerling, Radiation effects in Semiconductors, 1976, Ed. N. B. Urli and J. W. Corbett, (Inst. Phys. Conf. Ser. No. 31. London, 1977) p. 221.

[17] K. L. Wang, *Appl. Phys. Lett.*, 36, 48(1980).
[18] 张玉峰，张丽珠，吴书祥，杜永昌，半导体学报 3, 251(1982).
[19] G. D. Watkins and J. W. Corbett, *Phys. Rev.*, 121, 1001(1961).
[20] J. W. Walker and C. T. Sah, *Phys. Rev.*, 7, 4587(1973).
[21] G. D. Watkins and J. W. Corbett, *Phys. Rev.*, 134, A1359(1964).
[22] J. Krynicki and J. C. Bourgoin, Defects and Radiation effects in Semiconductors, 1978 (Inst of Phys. Conf. Ser. No. 46. London, 1979), p. 482.
[23] P. M. Mooney et al., *Phys. Rev.*, B15, 3836(1977).
[24] A. Mitic, T. Sato, M. Nishi and H. Hashimoto, *Appl. Phys. Lett.*, 37, 1727(1980).
[25] D. B. Jackson and C. T. Sah, J. Appl. Phys., 58, 1270(1985).
[26] D. B. Jackson and C. T. Sah, J. Appl. Phys., 59, 459(1986).

CALCULATIONS OF COMPOSITIONAL VARIATIONS OF ENERGY GAPS FOR ALLOYS BY CPA METHOD USING LCAO

Beijing BANDAOTI XUEBAO [CHINESE JOURNAL OF SEMICONDUCTORS] in Chinese
Vol 7 No 4, Jul 86 pp 380-386

[English abstract of article by Lu Fen [7120 1164] of the Modern Physics Institute, Fudan University]

[Text] Compositional variations of energy gaps for A_xB_{1-x}-type alloys, such as $GaAs_xP_{1-x}$, are calculated by the coherent-potential approximation method based on a tight-binding approximation using LCAO. Zero-order approximation is taken from the virtual-crystal approximation. The results obtained for $GaAs_xP_{1-x}$ agree well with the experimental results and the theoretical results from Chen and Sher. It is possible that the method can be used for studying other A_xB_{1-x}-type alloys. In addition, the energy bands and densities of state can also be calculated by this method. (Paper received 14 May 1985.)

REFERENCES

[1] Chen A. B. and Sher A., *Phys. Rev. Letters*, 40, 902(1978).
[2] Chen A. B. and Sher A., *Phys. Rev.*, B17, 4726(1978).
[3] Chen A. B. and Sher A., *Phys. Rev.*, B23, 5360(1981).
[4] Mariette H., Chevallior J. and Leroux-Hugon P., *Phys. Rev.*, B21, 5706(1980).
[5] Bugajski M. and Kontkiewicz A. M. and Mariette H., *Phys. Rev.*, B28, 7108(1983).
[6] Ehrenreich H. and Hass K. C., *J. Vac. Sci. Technol.*, 21, 133(1982).
[7] Chen A. B. and Sher A., *J. Vac. Sci. Technol.*, 21, 138(1982).
[8] Slater J. C. and Koster G. F., *Phys. Rev.*, 94, 1498(1954).
[9] Economou E. N., Green's Function in Quantum Physics, Spring-Verlag Berlin Heidelberg New York 1979.
[10] Yuan Li and Lin-Chung P. J. 未发表
[11] Ley L., Pollak R. A., Mcfeely F. R., Kowalczyk S. P. and Shirley D. A., *Phys. Rev.*, B9, 600 (1974).
[12] Eastman D. E., Grobman W. D., Freeouf J. L. and Erbudak M., *Phys. Rev.*, B9, 3473(1974).
[13] Thompson A. G. and Woolley J. C., *Phys. Rev.*, 146, 601(1966).

PLACEMENT SUBSYSTEM OF THE LSIS-II LAYOUT AUTOMATED SYSTEM

Beijing BANDAOTI XUEBAO [CHINESE JOURNAL OF SEMICONDUCTORS] in Chinese
Vol 7 No 4, Jul 86 pp 412-418

[English abstract of article by Cheng Kexing [4453 0668 5887], et al., of the Institute of Semiconductors, Chinese Academy of Sciences]

[Text] The modular placement subsystem for a standard cell with a macrocell is presented. The design can be in the batch or interactive way. In order to regulate the process of the placement, every module is reenterable. As macrocells are introduced, the layout of the circuit with RAM, ROM, PLA and gate matrix will be feasible, and the hierarchical design will be realized. The multiple objective function and multilevel iterative method are adopted in improvement placement. (Paper received 16 April 1985.)

REFERENCES

[1] 程可行，庄文君，半导体学报 5，422(1984).
[2] G. Persky, D. N. Deutsch and D. G. Schweikert, 13th D. A. Conf., pp399—407 (1976).
[3] S. Horiguchi, et al., IEEE Int. Solid-State Circuits Conf., 54(1982).
[4] B. T. Preas and C. W. Gwyn, 15th D. A. Conf., pp. 206—212 (1978)
[5] G. Persky et al., 18th D. A. Conf., pp. 22—29 (1981).
[6] H. Beke and W. Sanser, 16th D. A. Conf., pp. 102—108 (1979).
[7] 庄文君，计算机学报 7，217(1984).
[8] 庄文君，李玉兴，LSI/VLSI 布图设计自动化，上海交通大学出版社(将出版).

APPLICATION OF B SPLINE FUNCTION DEVICE INTERPOLATION MODELING IN CIRCUIT SIMULATION PROGRAM SPICE

Beijing BANDAOTI XUEBAO [CHINESE JOURNAL OF SEMICONDUCTORS] in Chinese
Vol 7 No 4, Jul 86 pp 419-426

[English abstract of article by Yan Zhixin [0917 1807 2450] of the Department of Physics, Shanghai University of Science and Technology; Wang Bijuan [3769 4310 1227], et al., of Shanghai Institute of Metallurgy, Chinese Academy of Sciences]

[Text] A new device interpolation modeling is added to SPICE (simulation program with integrated circuit emphasis) circuit simulation program by introducing into it a one to three-dimensional second-order B spline function. Therefore, the device simulation function in SPICE is extended and the circuit simulation accuracy in SPICE is enhanced. The characteristic simulation results of the tunnel diode oscillator and the 3 μm E/E NMOS circuit when using this modified SPICE program demonstrate the above-mentioned superiority of this new device modeling. Shanghai Computing Institute's IBM 370/148 was used in this work. (Paper received 29 April 1985.)

REFERENCES

[1] A. Vladimirescu and S. Liu, ERL Memo No. ERL M80/7, Electronics Research Laboratory, Univ. of California, Berkeley, Feb. 1980.
[2] [美]阿·弗拉吉米列斯科等, "SPICE 通用电路模拟程序用户指南",清华大学出版社(1983).
[3] 严志新,半导体学报, 6,113(1985).
[4] L. W. Nagel, ERL Memo No. ERL-M520, Electronics Research Laboratory, Univ. of California, Berkeley, May 1975.
[5] A. Vladimirescu, K. H. Zhang *et al.*, SPICE 2G.5 源程序版本附例, Aug. 1981.
[6] 孙家昶,"样条函数与计算几何",科学出版社(1982).
[7] Z. X. Yan and H. C. Lin, Presented at the Joint SIAM, IEEE Conference on Numerical Simulation of VLSI Device, Boston, Nov. 1982.

PHOTOELECTRON SPECTROSCOPY OF OXYGEN ADSORPTION ON a-GaAs(:H) SURFACE

Beijing BANDAOTI XUEBAO [CHINESE JOURNAL OF SEMICONDUCTORS] in Chinese
Vol 7 No 4, Jul 86 pp 433-436

[English abstract of article by Wang Zhaoping [3076 0340 1627] of the Institute of Semiconductors, Chinese Academy of Sciences]

[Text] The photoelectron spectroscopy of a-GaAs(:H) films after being exposed to excited oxygen is presented for the first time. The samples are prepared in situ by d.c. sputtering in a mixture of Ar and H_2. Two oxygen induced structures, a peak at 4.7 eV and a weak structure at 7-9 eV below the valence band maximum, are observed. Comparing these with the results of oxygen adsorption on the crystalline GaAs surface we presume that only dissociated oxygen is adsorbed on the surface of a-GaAs(:H). (Paper received 15 April 1985.)

REFERENCES

[1] W. Ranke and K. Jacobi, *Surf. Sci.*, 81(1979) 504.
[2] W. Ranke, Y. R. Xing and G. D. Shen, *Surf. Sci.*, 122(1982) 256.
[3] P. Pianetta, I. Lindau, P. E. Gregory, C. M. Garner and W. E. Spicer, *Surf. Sci.*, 72(1978), 298.
[4] C. Y. Su, I. Lindau, P. W. Chye, P. R. Skeath and W. E Spicer, *Phys. Rev.*, B25(1982) 4045.
[5] L. Ley, H. Richter, R. Kärcher, R. J. Johnson and J. Reichardt, *J. Physique*, 42(1981) C4-753.
[6] R. Kärcher, Z. P. Wang and L. Ley, J. Non-Gryst. Solids, 59/60(1983), 629.

9717
CSO: 4009/1123

END